mode frequency, equivalent viscous damping ratio and mode shapes were measured in the as-built condition of the structure and at the conditions after 1.5% and 3.0% overall drift ratio. The yield mechanism in the structure could have been developed at overall drift ratios between 0.5% and 2.0% (Figure 4-2).

Displacements of dynamic tests were bounded by a maximum overall drift ratio of 0.006% in the as-built condition and 0.14% in the other conditions. A proposed limit for small displacements in reinforced concrete structures was defined by an overall drift ratio of 0.03%. This limit was assumed also to be an elastic level of the structure, based on the negligible permanent deformation (no more than 0.006‰ overall drift ratio) observed at the end of dynamic tests performed at small displacements. Consequently, it is assumed that observation of different natural frequencies at different small displacements is caused by the nonlinear elastic behavior of the building. A finite-element model built using a commercial software and with gross section properties and modulus of elasticity according to ACI 2002, matched within 5% the observed fundamental frequency and mode shape of the structure in the as-built condition. The fundamental mode frequency was observed to be sensitive to the level of displacements in the dynamic tests even in the elastic behavior range. Ratios between frequency and equivalent viscous damping ratio values estimates in the as-built condition and after 3.0% overall drift ratio were 2.0 and 0.4, respectively. The fundamental frequency dropped by 20% from the condition after 1.5% drift ratio to the condition after 3.0% drift ratio. A punching-shear failure was observed in the building at the drift ratio of 3.0%.

Experimental program in the small-scale beams consisted of free, forced and ambient vibration tests at small displacements (maximum overall drift ratio of 0.03%). The small displacements corresponded to displacement levels below the cracking displacement of the beam and therefore were assumed to be elastic levels of the system. Natural frequency, mode shape and equivalent viscous damping ratio were measured in the as-built condition and after pseudo-static loading cycles with overall drift ratios of 0.4%, 1.1%, 1.8%, 2.7%, 3.6%, 5.4%, 7.1%, 8.9%, 10%, and 13%. The drift ratio associated with the yield displacement of the beams was 1.8%. Natural frequency and damping ratio were found to be sensitive to elastic displacements of the tests. A mean frequency reduction factor of 2.2 from initial condition to the condition after 1.8% drift ratio was found (Figure 4-29 and Figure 4-33). Additional reduction of frequency after 1.8% drift ratio was seen to be in the order of 20% of the total reduction observed. Equivalent viscous damping ratio increased from its initial-condition value with the first displacement demand levels (Figure 4-30 and Figure 4-34). Maximum values of damping ratio were reached in the vicinity of condition of 1.8% overall drift ratio. Larger displacement demands caused reduction in the damping ratio.

### 7.1.3. Analytical tools

Nonlinear elastic behavior of the reinforced concrete structures was assessed by using Fourier and Hilbert transform analyses. While the Fourier approach was used to determine frequency predominance in the full response, the Hilbert transform was used to track vibration frequency of the system over time. A method to extract load versus displacement curve from free vibration records was presented. In the method, only estimates of frequency at peak-displacement instants (zero velocity) were used. Full description of the load-displacement curve was completed by linear interpolation between the values computed at peak displacements. The method was verified with records from the full-scale structure of chapter 4 (Figure 5-5).

### 7.1.4. Observations from other experiments behavior

Identified behavior of frequency and damping with displacement from the experimental program was compared with those observed in experiments done by other researches. Observations from the full-scale 3-story structure and the six small-scale beams of chapter 4 were compared to those from 36 other experiments. The reinforced concrete structures used for comparison were distributed as follows (Table 6-25): 14 small-scale frame/frame-wall buildings, 3 slab-column connections, 1 full-scale frame-wall building, 4 small-scale beams, 1 full-scale wall building, one system made up with slab-column + frame system and 12 single-degree-of-freedom specimens. Reinforcing ratios of columns, beams, walls and slabs of those structures ranged from 0.4% to 3.5%, from 0.4% to 2.6%, from 0.6% to 1.5% and from 0.7% to 1.3%, respectively. In some of those structures, frequency and damping ratio had been obtained from free vibration tests conducted at similar initial pull force (specimens of Table 6-1 and Figure 6-3) resulting in different initial displacements. In order to track variation of equivalent viscous damping ratio measured at an identical displacement level, damping ratio values normalized according to equation 6.1 were computed for the structures of Table 6-1 and Figure 6-3.

Estimates of frequency and damping ratio variations were compared with those observed in a 7-story wall building that was subject to different base motions (Panagiotou 2008). Frequency and damping ratio estimated from white-noise tests were compared to those values obtained from earthquake response records (Table 6-23). In an attempt to do a fair comparison, estimates from small-amplitude (white-noise) tests were compared with estimates from the smaller-amplitude portions of the earthquake records (beginning or end of record). Damping ratio values estimated from earthquake records lied between 0.4 and 2.3 times the values estimated from white-noise tests. Ratio between frequency values from earthquake records and values from white-noise tests lied between 1.0 and 1.4.

## 7.2. Conclusions

Based on the experiments on the full-scale 3-story building, small-scale cantilever beams, and review and comparison with other evidence the following conclusions are made:

1. Fundamental-mode frequency and equivalent viscous damping ratio at small displacement (0.03% overall drift ratio) are sensitive to past levels of deformations in reinforced concrete structures.

2. Fundamental frequency and equivalent viscous damping ratio are amplitude-dependent parameters even at small displacements (0.03% drift ratio). This is a consequence of nonlinear elastic behavior of reinforced concrete structures.

3. A reinforced concrete structure with a normal reinforcing ratio (about 1%) is likely to have a reduction of its initial fundamental frequency by a factor larger than 1.5 after 1.5% overall drift ratio (Figure 6-6).

4. Equivalent viscous damping ratio measured at a given small displacement increases with increase in the past maximum displacement, until approximately the yield displacement of the reinforced concrete structure. Further increases of past maximum displacement in the structure causes a reduction of the equivalent viscous damping ratio measured at the given small displacement.

5. Vibration tests before and after a past-maximum-displacement event need to be made at similar drift levels. If tests are made at different drift levels, the equivalent viscous damping ratios and natural frequency need to be adjusted (normalized) to similar drift levels, if possible. A rigorous procedure to adjust those estimates should consider the effect of variable stiffness and variable damping at small displacements in reinforced

concrete structures. The normalization procedure for a given structure may be different from the one considered in this study.

6. Current observations regarding variation of fundamental frequency and equivalent viscous damping with maximum past drift levels in reinforced concrete structures may be used in monitoring the state of a structure, as in structural health monitoring before and after an earthquake.

7. There is a need for low amplitude vibration test data to verify if the combined behavior of fundamental frequency and equivalent viscous damping ratio observed in small scale test specimens applies in full scale structures.

## 7.3. Future work

Variation of dynamic parameters estimated at small displacement response levels with past maximum deformation level is of interest in the field of structural health monitoring. More data from full-scale reinforced concrete structures is needed to verify the presence of the behavior of damping observed in small-scale structures. Observations at low drift levels, i.e., before a yield mechanism in the structure is formed, are necessary in order to verify the increase and then decrease of damping ratio at low response with past maximum drift level.

In this study, nonlinear elastic and variable equivalent viscous damping model is used to represent the load-resisting nature and collective effect of energy dissipating mechanisms of a structure. It is possible that damping mechanisms other than viscous damping, such as Coulomb damping and hysteretic damping, may exist in a structure and may vary in proportion depending on the state of the structure. These other damping mechanisms may influence the accuracy of the model considered in this study. It would be worth studying the possible presence and contribution of various damping mechanisms separately –in particular, with an eye to investigate how they vary with past maximum deformation level in a structure. It is important to keep in mind that when one is trying to deduce critical changes in the state of a structure using observations made during small amplitude vibration levels, assumptions that are typical and acceptable at other times may not be applicable.

It is possible that the variation of dynamic parameters depends on the number of cycles at or near the past peak displacement. This possibility needs to be investigated using controlled laboratory tests

Extension of the proposed method to calculate load versus displacement curves can be done. Methods that consider the actual inelastic response of reinforced concrete structures would help in determine the true load-displacement curves from response recorded during actual earthquakes. Methods that can determine the characteristics of the system in only one full-cycle of motion are also desired. Such methods would allow using the usually limited amount of data collected during earthquake records.

REFERENCES

# REFERENCES


Abrams, D. P., and Sozen, M. A. (1979). "Experimental Study of Frame-Wall Interaction in Reinforced Concrete Structures Subjected to Strong Earthquake Motions." *Civil Engineering Studies, Structural Research Series (University of Illinois at Urbana-Champaign, Department of Civil Engineering)*(460).

ACI. (2002). "Building Code Requirements from Structural Concrete and Commentary." ACI Committee 318, Farmington Hills, Michigan.

Arboleda-Monsalve, L. G. (2006). "Small-amplitude Vibration Tests of a Full-scale Reinforced-concrete Flat-plate Structure," Master Thesis, Purdue University, West Lafayette.

ASTM_C-469. "Test Methods for Static Modulus of Elasticity and Poisson's Ratio of Concrete in Compression." Annual Book of ASTM Standards.

Bendat, J. S., and Piersol, A. G. (1986). *Random data : analysis and measurement procedures*, Wiley, New York.

Bert, C. W. (1973). "Material Damping: An Introductory Review of Mathematical Models, Measures and Experimental Techniques." 29(2), 129-153.

Bonacci, J. F. (1989). "Experiments to study the seismic drift of reinforced concrete structures," Doctoral Thesis, University of Illinois, Urbana.

Bousman, W. G., and Winkler, D. J. (1981). "Application of the Moving-Block Analysis." *Collection of Technical Papers - AIAA/ASME/ASCE/AHS Structures, Structural Dynamics & Materials Conference*(Pt 2, ad), 755-763.

Bradford, S. C. (2006). "Time-frequency analysis of systems with changing dynamic properties," Doctoral Thesis, California Institute of Technology.

Celebi, M. (1996). "Comparison of damping in buildings under low-amplitude and strong motions." *Journal of Wind Engineering and Industrial Aerodynamics*, 59(2-3), 309-323.

Chang, P. C., Flatau, A., and Liu, S. C. (2003). "Review Paper: Structural Health Monitoring of Civil Infrastructure." *Structural Health Monitoring*(2, 3), 257-267.

Chopra, A. K. (1995). *Theory and Applications to Earthquake Engineering*, Prentice-Hall, Inc., NJ.

Clinton, J. F., Bradford, S. C., Heaton, T. H., and Favela, J. (2006). "The observed wander of the natural frequencies in a structure." *Bulletin of the Seismological Society of America*, 96(1), 237-257.

Clough, R. W., and Penzien, J. (1975). *Dynamics of structures*, McGraw-Hill, New York.

Cole, H. A., Jr. (1973). "On-Line Failure Detection and Damping Measurement of Aerospace Structures by Random Decrement Signatures." *NASA Contractor Reports*, 77.

Computers and Structures, I. (2003). "SAP2000." Berkeley, CA, Static and Dynamic Finite Element Analysis of Structures.

Curadelli, R. O., Riera, J. D., Ambrosini, R. D., and and Amani, M. G. (2007). "Damping: A Sensitive Structural Property for Damage Detection." Proc. XVI Congress on Numerical Methods and their Applications, ENIEF 2007, Cordoba, Argentina.

Deering, R., and Kaiser, J. F. (2005). "The use of a masking signal to improve Empirical Mode Decomposition." *ICASSP, IEEE International Conference on Acoustics, Speech and Signal Processing - Proceedings*, IV, IV485-IV488.

Dieterle, R., and Bachman, H. (1981). "Experiments and Models for the Damping Behavior of Vibrating Reinforced Concrete Beams in the Uncracked and Cracked Conditions." *Reports of the Working Commissions (International Association for Bridge and Structural Engineering*, 34, 69-82.

Doebling, S. W. (1996). "Damage identification and health monitoring of structural and mechanical systems from changes in their vibration characteristics: a literature review." Los Alamos laboratory, New Mexico.

Doebling, S. W., Farrar, C. R., and Prime, M. B. (1998). "Summary review of vibration-based damage identification methods." *Shock and Vibration Digest*, 30(2), 91-105.

Donnelly, D., and Rust, B. (2005). "The fast Fourier transform for experimentalists." *Computing in Science and Engineering*, 7(3), 71.

Eberhard, M. O., and Sozen, M. A. (1989). "Experiments and Analyses to Study the Seismic Response of Reinforced Concrete Frame-Wall Structures with Yielding Columns." *Structural Research Series*(548).

Feldman, M. (2006). "Time-varying vibration decomposition and analysis based on the Hilbert transform." *Journal of Sound and Vibration*, 295(3-5), 518-530.

Feldman, M. (2007). "Considering high harmonics for identification of non-linear systems by Hilbert transform." *Mechanical Systems and Signal Processing*, 21(2), 943-958.

Fick, D. (2008). "Experimental Investigation and Analytical Modeling of the Nonlinear Response of Flat-Plate Structures Subjected to Cycling Loading Failure," Doctoral Thesis, School of Civil Engineering, Purdue University.

Flandrin, P., and Stöckler, J. (1999). *Time-Frequency/Time-Scale Analysis*, Academic Press, Paris.

Flesch, R. (1981). "Damping Behavior of R/C Cantilever Elements." *Reports of the Working Commissions (International Association for Bridge and Structural Engineering*, 34, 83-98.

Galambos, T. V., and Mayes, R. L. (1978). "Dynamic Tests of a Reinforced Concrete Building." Washington University.

Gao, Y., Spencer, B. F., and Bernal, D. (2007). "Experimental verification of the flexibility-based damage locating vector method." *Journal of Engineering Mechanics*, 133(10), 1043-1049.

Gulkan, P., and Sozen, M. A. (1977). "Inelastic Responses of Reinforced Concrete Structures to Earthquake Motions." *Publication SP - American Concrete Institute*, 109-115.

Hall, J. F., Heaton, T. H., Halling, M. W., Wald, a., and J., D. (1995). "Near-Source Ground Motion and Its Effects on Flexible Buildings." *Earthquake Spectra*, 11(4), 37.

Healey, T. J., and Sozen, M. A. (1978). "Experimental Study of the Dynamic Response of a Ten-Story Reinforced Concrete Frame with a Tall First Story." *Structural Research Series*(450).

Huang, N. E., Shen, Z., Long S. R., W. M. C., Shih, H. H., Zheng, Q., Yen, N., Tung, C. C., and and Liu, H. H. (1998). "The Empirical Mode Decomposition and the Hilbert Spectrum for Nonlinear and Non-stationary Time Series Analysis." Vol. 454, 903-995.

Ivanovic, S. S., Trifunac, M. D., and I., a. T. M. (1999). "On Identification of Damage in Structures Via Wave Travel Times." Proc. Nato Advance Research Workshop on Strong-Motion Instrumentation for Civil Engineering Structures, Istanbul, Turkey, Kluwer Publ.

Ivanovic, S. S., Trifunac, M. D., Novikova, E. I., Gladkov, A. A., and Todorovska, M. I. (2000). "Ambient vibration tests of a seven-story reinforced concrete building in Van Nuys, California, damaged by the 1994 northridge earthquake." *Soil Dynamics and Earthquake Engineering*, 19(6), 391-411.

Iwan, W. D., and Gates, N. C. (1979). "Effective Period and Damping of a Class of Hysteretic Structures." *Earthquake Engineering & Structural Dynamics*, 7(3), 199-211.

Jeary, A. P. (1997). "Damping in structures." *Journal of Wind Engineering and Industrial Aerodynamics*, 72(1-3), 345-355.

Kaminoso, T., Okamoto, S., Kitagawa, Y., and Yoshimura, M. (1985). "Testing Procedure and Preliminary Tests results of a Full Scale Seven Story Reinforced Concrete Building." American Concrete Institute.

Kimball, A. L., and Lovell, D. E. (1927). "Internal friction in solids." *Physical Review*, 30(6), 948-959.

Kohler, M. D., Heaton, T. H., and Bradford, S. C. (2007). "Propagating waves in the steel, moment-frame factor building recorded during earthquakes." *Bulletin of the Seismological Society of America*, 97(4), 1334-1345.

Kwok, K. C. S., Apperley, L. W., Matesic, I. J., and Mangion, C. B. (1990). "Measurement of natural frequencies of vibration and damping ratios of tall buildings and structures." *National Conference Publication - Institution of Engineers, Australia*(90 pt 10), 23-27.

Lakshmanan, N., Srinivasulu, P., and Parameswaran, V. S. (1991). "Post cracking stiffness and damping in reinforced concrete beam elements." *Journal of Structural Engineering (Madras)*, 17(4), 105-105.

Lazan, B. J. (1968). *Damping of materials and members in structural mechanics*, Oxford, New York, Pergamon Press.

Li, Q. S., Yang, K., Zhang, N., Wong, C. K., and Jeary, A. P. (2002). "Field measurements of amplitude-dependent damping in a 79-storey tall building and its effects on the structural dynamic responses." *Structural Design of Tall Buildings*, 11(2), 129-153.

Mallat, S. (1999). *A wavelet tour of signal processing*, Academic Press, San Diego.

Messina, A., Williams, E. J., and Contursi, T. (1998). "Structural damage detection by a sensitivity and statistical-based method." *Journal of Sound and Vibration*, 216(5), 791-808.

Mitchell, D., DeVall, R. H., Saatcioglu, M., Simpson, R., Tinawi, R., and Tremblay, R. (1995). "Damage to concrete structures due to the 1994 Northridge earthquake." *Canadian journal of civil engineering*, 22(2), 361-377.

Modena, C., Sonda, D., and Zonta, D. (1999). "Damage localization in reinforced concrete structures by using damping measurements." *Key Engineering Materials*, 167-168, 132-141.

Moehle, J. P., and Sozen, M. A. (1978). "Earthquake-Simulation Tests of a Ten-Story Reinforced Concrete Frame with a Discontinued First-Level Beam." *Structural Research Series*(451).

Moehle, J. P., and Sozen, M. A. (1980). "Experiments to Study Earthquake Response of R/C Structures with Stiffness Interruptions." *Civil Engineering Studies, Structural Research Series (University of Illinois at Urbana-Champaign, Department of Civil Engineering)*(482).

Morrison, D. G., and Sozen, M. A. (1981). "Response of Reinforced Concrete Plate-Column Connections to Dynamic and Static Horizontal Loads." *Civil Engineering Studies, Structural Research Series (University of Illinois at Urbana-Champaign, Department of Civil Engineering)*(490), 249.

Myklestad, N. O. (1952). "Concept of complex damping." *American Society of Mechanical Engineers -- Transactions -- Journal of Applied Mechanics*, 19(3), 284-286.

Nashif, A. D., Jones, D. I. G., and Henderson, J. P. (1985). *Vibration damping*, New York : Wiley, 1985.

Oppenheim, A. V., Schafer, R. W., and Buck, J. R. (1999). *Discrete-Time Signal Processing*.

Panagiotou, M. (2008). "Seismic Design, Testing and Analysis of Reinforced Concrete Wall Buildings," Doctoral Thesis, University of California, San Diego.

Peters, J. M. H. (1995). "A beginner's guide to the Hilbert transform." *International Journal of Modern Physics*, 10(8), 89.

Pujol, S. (2002). "Drift Capacity of Reinforced Concrete Columns Subjected to Displacement Reversals," PhD Thesis, Purdue University, West Lafayette.

Safak, E. (1999). "Wave-propagation formulation of seismic response of multistory buildings." *Journal of Structural Engineering*, 125(4), 426-437.

Salawu, O. S. (1997). "Detection of structural damage through changes in frequency: A review." *Engineering Structures*, 19(9), 718-723.

Scanlan, R. H., and Meldenson, A. (1962). "Structural Damping." *American Institute of Aeronautics and Astronautics Journal*, Vol. 1, No. 4.

Shi, Z. Y., Law, S. S., and Zhang, L. M. (2006). "Damage Location by directly using incomplete Mode Shapes." *Journal of Engineering Mechanics, ASCE*, Vol. 126(No. 6).

Snieder, R., and Safak, E. (2006). "Extracting the building response using seismic interferometry: Theory and application to the Millikan Library in Pasadena, California." *Bulletin of the Seismological Society of America*, 96(2), 586-598.

Sohn, H., Farrar, C. R., Hemez, F. M., Shunk, D. D., Stinemates, D. W., and and Nadler, B. R. (2003). "A review of structural health monitoring literature: 1996-2001." Los Alamos laboratory, Massachussetts Institure of Technology.

Soroka, W. W. (1949). "Note on relations between viscous and structural damping coefficients." *Journal of the Aeronautical Sciences*, 16(7), 409-410.

Takeda, T., Sozen, M., and Nielsen, N. N. (1970). "Reinforced Concrete Response to Simulated Earthquakes." *Journal of the Structural Division - Proceedings of the American Society of Civil Engineers*.

The MathWorks, I. (2004). "MATLAB, The Language of Technical Computing."

Todorovska, M. I., and Trifunac, M. D. (2008a). "Earthquake damage detection in the Imperial County Services Building III: Analysis of wave travel times via impulse response functions." *Soil Dynamics and Earthquake Engineering*, 28(5), 387-404.

Todorovska, M. I., and Trifunac, M. D. (2008b). "Impulse response analysis of the Van Nuys 7-storey hotel during 11 earthquakes and earthquake damage detection." *Structural Control and Health Monitoring*, 15(1), 90-116.

Trifunac, M. D. (1972). "Comparison between ambient and forced vibration experiments." *Earthquake Engineering and Structural Dynamics*, 1, 133-150.

Trifunac, M. D., Ivanovic, S. S., and Todorovska, M. I. (2003). "Wave propagation in a seven-story reinforced concrete building. III. Damage detection via changes in wavenumbers." *Soil Dynamics and Earthquake Engineering*, 23(1), 65-75.

Ville, J. (1948). "Theorie et applications de la notion de signal analytique." *Cables et Transmissions*, 2A(1), 61—74. I. Selin, translator.

Wegel, R. L., and Walther, H. (1935). "Internal Dissipation in Solids for Small Cyclic Strains." *Physics*, Vol. 6, 141-157.

Westergaard, H. M. (1933). "Earthquake-shock transmission in tall buildings." *Engineering News-Record*, 111(22), 654-656.

Wigner, E. P. (1932). "On the quantum correction for thermodynamic equilibrium." *Physical Review*(40), 749—759.

Wood, S. L. (1985). "Experiments to Study the Earthquake Response of Reinforced Concrete Frames with Setbacks," Doctoral Thesis, University of Illinois, Urbana.

Wu, Z., Liu, H., Liu, L., and Yuan, D. (2007). "Identification of nonlinear viscous damping and Coulomb friction from the free response data." *Journal of Sound and Vibration*, 304(1-2), 407-414.

Wyatt, T. A. (1977). "Mechanisms of Damping." *TRRL Supplementary Report (Transport and Road Research Laboratory, Great Britain)*(275), 10-21.

Yang, J. N., Lei, Y., Lin, S., and Huang, N. (2004). "Hilbert-Huang based approach for structural damage detection." *Journal of Engineering Mechanics*, 130(1), 85-95.

Yu, E. (2005). "Forced Vibration Testing and Analytical Modeling of a Four-story Reinforced Concrete Frame Building," Doctoral Thesis, University of California, Los Angeles.

# APPENDICES

# Appendix A.
## Location and properties of sensors used in the full-scale 3-story flat-plate building

Data collection in the full-scale 3-story building was done by means of a data acquisition system consisted of an 18-bit, 500kS/s (multi-channel) card (NI PCI-6289) and a network of LVTDs and accelerometers. Figure A-1 and Table A-1 show the location and the properties of the sensors respectively. Sensor orientations for tests in the NS direction are identified by arrows. One LVDT at a time was placed on the south edge of the each slab-floor. Two LVDTs were interchanged at second floor and the roof according to precision and range demands of tests. A capacitive-based accelerometer was located at center of slab of each floor. Accelerometer A4 not shown in the Figure A-1 was placed on top of the linear-vibrating mass used for forced vibration tests. Mid-west column was densely instrumented by use of seven piezoelectric-accelerometers. One piezoelectric-based accelerometer was located at mid-height of first, second and third story. Inclinometers to measure rotation on the slab about an axis parallel to EW direction were used at each slab-floor. One inclinometer was placed at the center of slab at each floor and another by the mid-west column on second floor and roof. Identical configuration to that of Figure A-1 was used for tests in the EW direction with proper alignment of sensors and without using LVDTs and inclinometers.

Table A-1 Properties of sensors installed on the full-scale structure

| | Sensor | Sensitivity constant | Units | Accuracy | Noise level |
|---|---|---|---|---|---|
| LVDTs | LVDT 1 | 39.477 | V/in | 0.001in | 3E-5in |
| | LVDT 1A | 194.65 | V/in | 0.0005in | 4E-5in |
| | LVDT 2 | 39.936 | V/in | 0.001in | 4E-5in |
| | LVDT 3 | 40.900 | V/in | 0.001in | 4E-5in |
| | LVDT 3A | 20.748 | V/in | 0.0005in | 2E-4in |
| Capacitive-based accels | A1 | 1,010 | mV/g | 0.05mg | 1.0mg |
| | A2 | 994 | mV/g | 0.04mg | 1.0mg |
| | A3 | 1,005 | mV/g | 0.04mg | 1.0mg |
| | A4 | 1,008 | mV/g | 0.04mg | 1.0mg |
| Piezoelectric-based accels | A5 | 1,061 | mV/g | 0.08mg | 5mg |
| | A6 | 1,048 | mV/g | 0.08mg | 5mg |
| | A7 | 1,077 | mV/g | 0.08mg | 5mg |
| | A8 | 1,060 | mV/g | 0.08mg | 5mg |
| | A9 | 1,051 | mV/g | 0.08mg | 5mg |
| | A10 | 1,045 | mV/g | 0.08mg | 5mg |
| | A11 | 960 | mV/g | 0.08mg | 5mg |
| | A12 | 1,040 | mV/g | 0.08mg | 5mg |
| Inclinometers | 1A | 28.9 | mV/deg | 0.001deg | 0.02deg |
| | 2A | 29.4 | mV/deg | 0.001deg | 0.02deg |
| | 3A | 28.0 | mV/deg | 0.001deg | 0.02deg |
| | 1B | 30.6 | mV/deg | 0.001deg | 0.02deg |
| | 3B | 28.8 | mV/deg | 0.001deg | 0.02deg |
| Load cells | Free vib. | 2,869 | mV/kip | 0.010kip | 0.002kip |
| | Forced Vib. | 2.00E-04 | mV/kip | 0.017kip | 0.002kip |

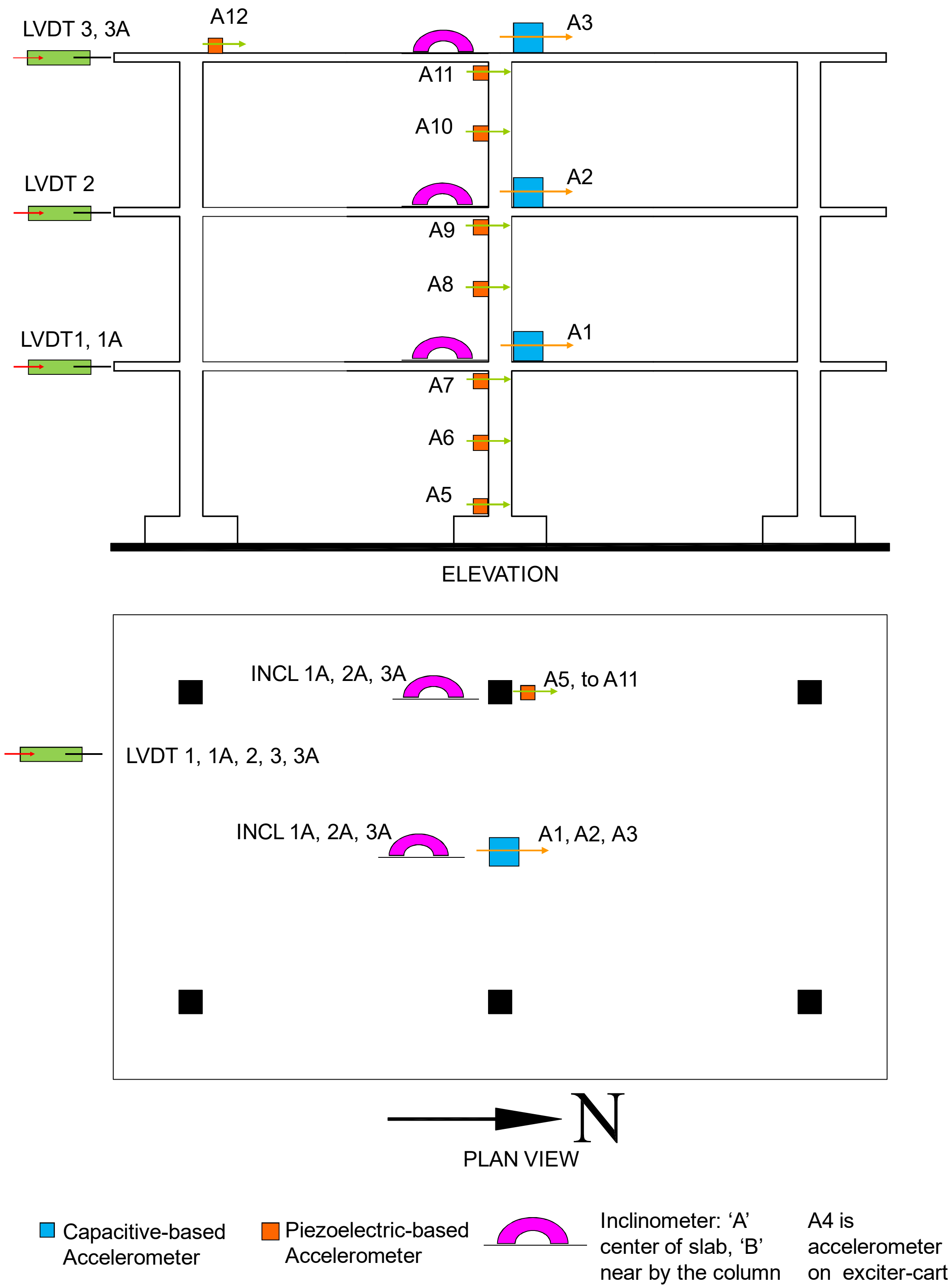


Figure A-1 Sensor layout on the full-scale structure.

# Appendix B.

## Dynamic tests in the full-scale 3-story flat-plate structure in the EW direction

Table B-1 Free Vibration summary by pull-release at roof level in the EW direction

| | | | | | Mode Shape | | | Damping | |
|---|---|---|---|---|---|---|---|---|---|
| | **Test** | $\Delta_{roof}$ **[in]** | **P [kip]** | **f [Hz]** | $\phi1$ | $\phi2$ | $\phi3$ | N (cycles) | $\zeta$ [%] |
| **As-built** | E 1-1 | 0.020 | 1.5 | 1.81 | 0.23 | 0.65 | 1.00 | 50 | 0.5 |
| | E 1-2 | 0.020 | 1.6 | 1.81 | 0.23 | 0.64 | 1.00 | 50 | 0.5 |
| | E 1-3 | 0.020 | 1.6 | 1.81 | 0.23 | 0.65 | 1.00 | 50 | 0.5 |
| **After 1.5% overall drift** | E 2-1 | 0.020 | 1.0 | 1.53 | 0.26 | 0.67 | 1.00 | 50 | 1.0 |
| | E 2-2 | 0.020 | 0.9 | 1.53 | 0.26 | 0.65 | 1.00 | 50 | 1.1 |
| | E 2-3 | 0.020 | 1.1 | 1.53 | 0.26 | 0.66 | 1.00 | 50 | 1.0 |
| | E 2-4 | 0.040 | 1.9 | 1.52 | 0.26 | 0.66 | 1.00 | 50 | 1.4 |
| | E 2-5 | 0.040 | 1.9 | 1.51 | 0.25 | 0.65 | 1.00 | 30 | 1.7 |
| | E 2-6 | 0.041 | 1.9 | 1.52 | 0.26 | 0.66 | 1.00 | 30 | 1.6 |
| **After 3.0% overall drift** | E 3-1 | 0.020 | 0.6 | 1.12 | 0.30 | 0.69 | 1.00 | 50 | 0.9 |
| | E 3-2 | 0.020 | 0.7 | 1.12 | 0.31 | 0.69 | 1.00 | 50 | 0.9 |
| | E 3-3 | 0.020 | 0.7 | 1.13 | 0.31 | 0.69 | 1.00 | 50 | 0.9 |
| | E 3-4 | 0.040 | 1.3 | 1.11 | 0.31 | 0.69 | 1.00 | 50 | 1.1 |
| | E 3-5 | 0.040 | 1.3 | 1.10 | 0.31 | 0.69 | 1.00 | 50 | 1.1 |
| | E 3-6 | 0.040 | 1.3 | 1.10 | 0.31 | 0.69 | 1.00 | 50 | 1.1 |
| | E 3-7 | 0.080 | 2.3 | 1.08 | 0.31 | 0.69 | 1.00 | 50 | 1.2 |
| | E 3-8 | 0.080 | 2.4 | 1.07 | 0.31 | 0.70 | 1.00 | 50 | 1.2 |
| | E 3-9 | 0.081 | 2.3 | 1.08 | 0.31 | 0.70 | 1.00 | 50 | 1.3 |

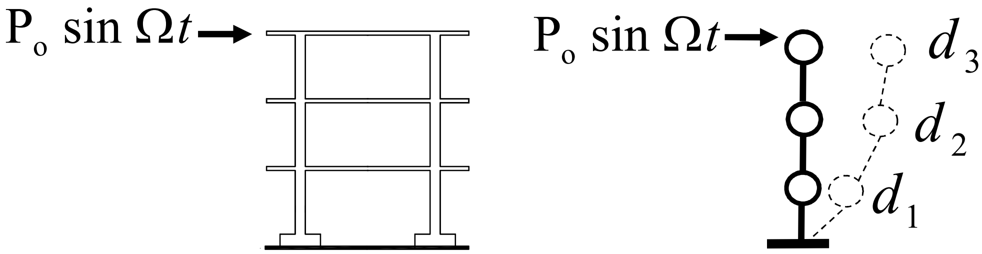


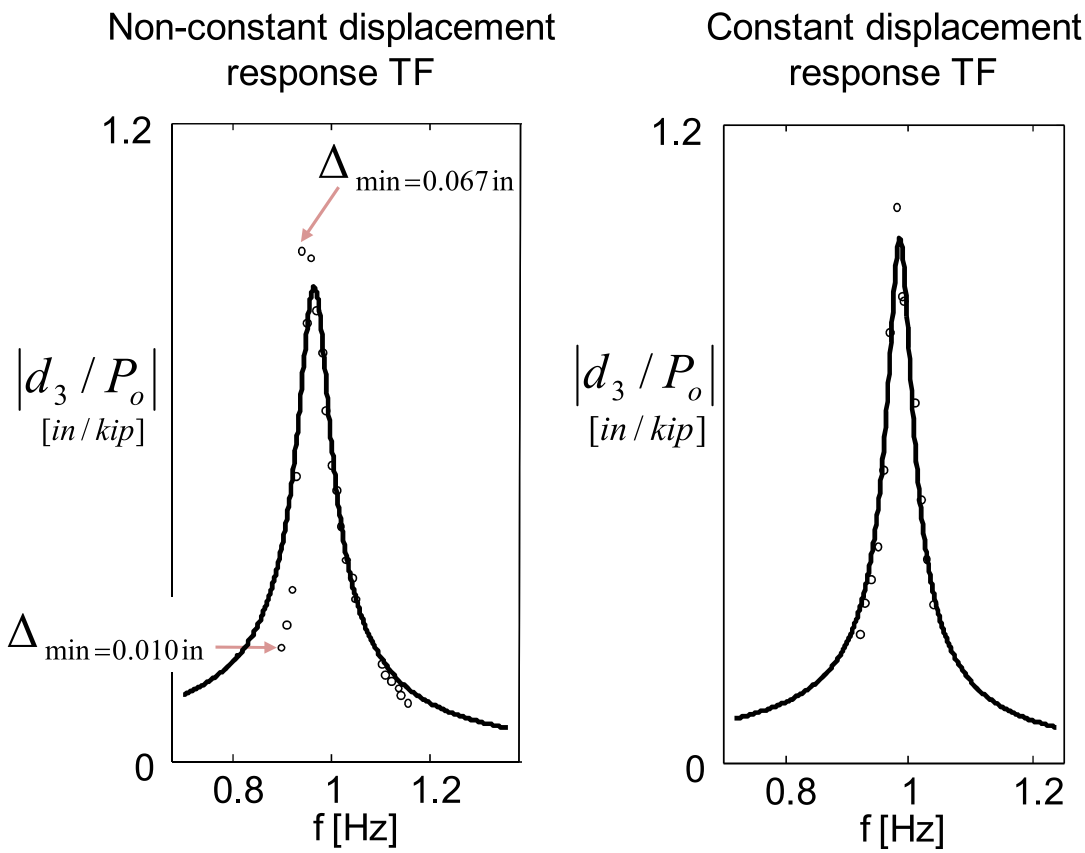


| | Δ roof [in] max | Δ roof [in] min | $f_1$ [Hz] | K roof [kip/in] | ζ [%] | Mode Shape 1 φ1 | Mode Shape 1 φ2 | Mode Shape 1 φ3 |
|---|---|---|---|---|---|---|---|---|
| **After 3.0% overall drift** | 0.067 | 0.010 | 0.97 | 17.0 | 3.3 | 0.27 | 0.58 | 1.00 |
| | 0.020 | | 0.99 | 26.3 | 1.9 | 0.26 | 0.58 | 1.00 |

Figure B-1 Forced vibrations on EW direction. After 3.0% overall drift ratio.

Appendix C.

Displacements from acceleration records in the full-scale 3-story flat-plate structure

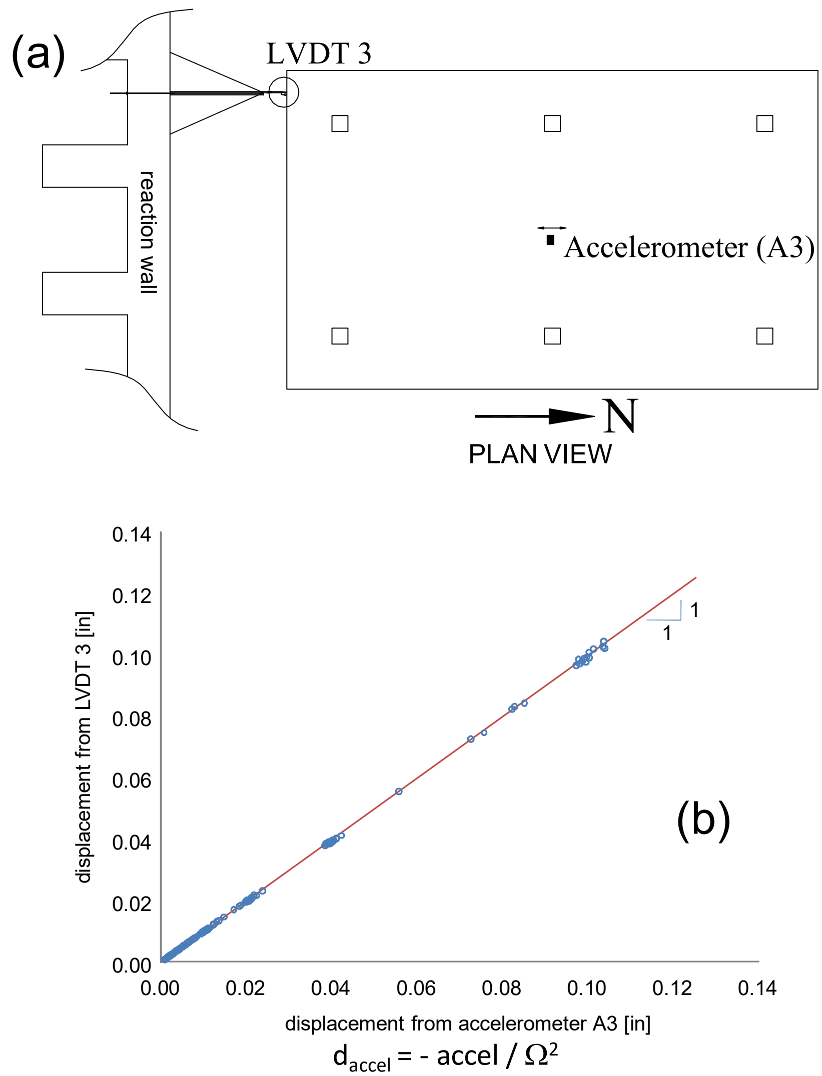


Figure C-1 Comparison of displacements measured by LVDT and those inferred from accelerations measured by accelerometer. (a) Location of sensors. (b) Comparison of displacements.

# Appendix D.
## Interaction of natural frequency of barrels full of water with second structure mode (tuned mass damper effect)

The natural frequency of the barrels, as illustrated in Figure D-1 (a) and (b), thus from free vibration and forced vibration tests respectively, was found to in the vicinity of the second-mode frequency of the full-scale building in the as-built condition, $f_2$ = 7.6 Hz (see Table 4-3). This condition caused a reduction of second-mode participation of the full-scale building. Figure D-1 (c) illustrates the location and sensors used during forced vibration in order to observe the response of the main structure (building) and the tuned-mass dampers (barrels). When the system is excited with an excitation frequency far away from the second-mode natural frequency of the building (and that of barrels), for example f = 2 Hz, the barrels vibrate in phase with the building as shown in Figure D-1 (d). In the other hand, when the excitation frequency used is around the second-mode frequency, vibrations in the building are minimized and vibrations of the barrels (out of phase with respect of vibrations of the building) are one order of magnitude larger than those of the building as shown in Figure D-1 (e).

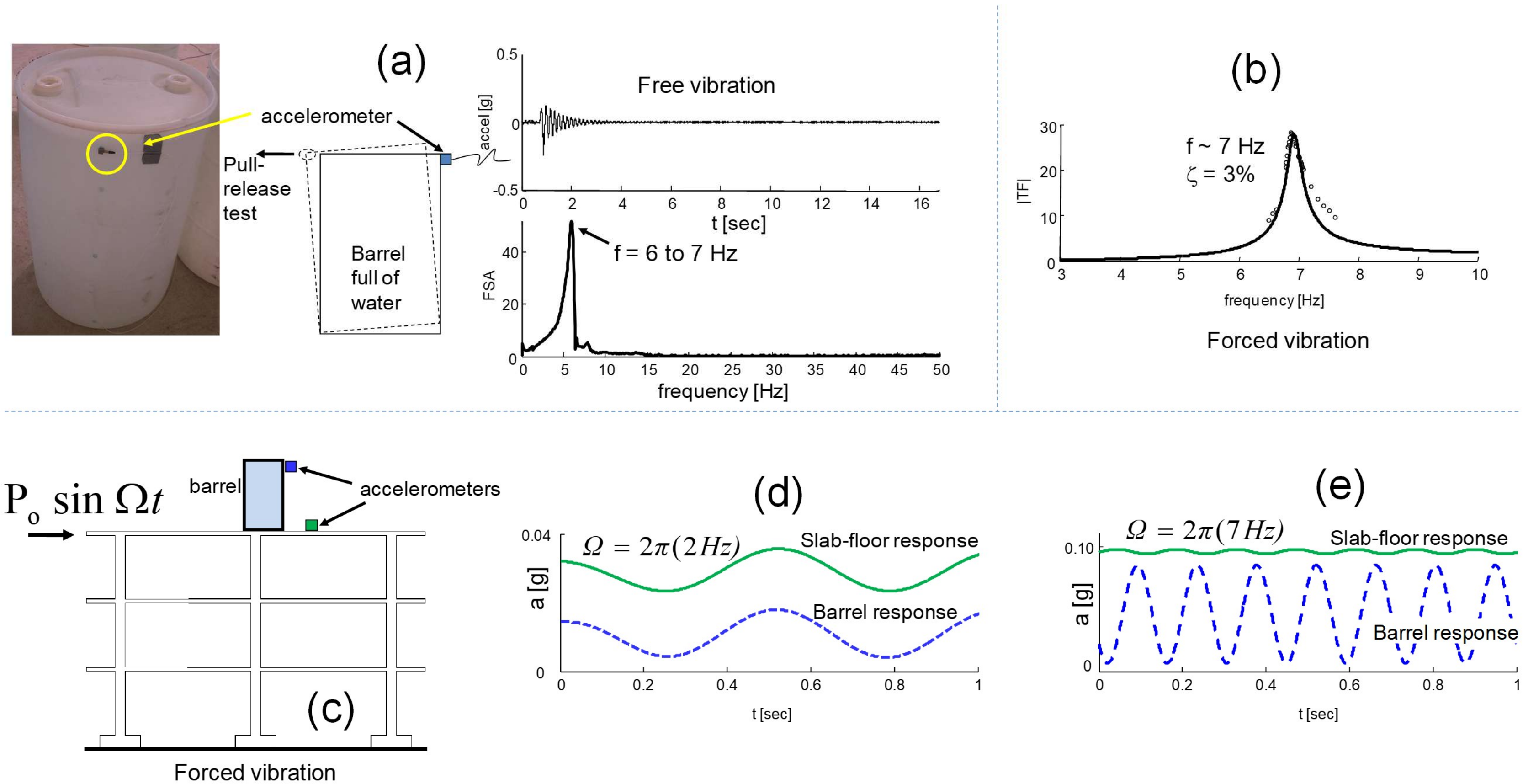


Figure D-1 Tuned-mass damper provided by barrels. (a) Free vibration response of barrel. (b) Transfer function of barrel. (c) Set-up of forced vibration tests. (d) Response of building and barrel when using an excitation frequency of 2 Hz. (e) Response of building and barrel when using an excitation frequency of 7 Hz.

# Appendix E.

## Additional information of the small-scale cantilever beams

Table E-1 Cylinder compressive strength tests

| | f'c [psi] | | | | | | | | |
|---|---|---|---|---|---|---|---|---|---|
| | Compressive Strength | | | Specimens | | | | | |
| **Cylinder** | **7 days** | **14 days** | **28 days** | **1** | **2** | **3** | **4** | **5** | **6** |
| A-1 | 2,200 | | | | | | | | |
| A-2 | 2,511 | | | | | | | | |
| A-3 | | 2,649 | | | | | | | |
| A-4 | | 2,387 | | | | | | | |
| A-5 | | | 2,833 | | | | | | |
| A-6 | | | 2,381 | | | | | | |
| A-7 | | | | 2,360 | | | | | |
| A-8 | | | | 3,699 | | | | | |
| A-9 | | | | | | 3,200 | | | |
| A-10 | | | | | | 3,529 | | | |
| A-11 | | | | | 3,481 | | | | |
| A-12 | | | | | 3,348 | | | | |
| B-1 | 3,082 | | | | | | | | |
| B-2 | 2,573 | | | | | | | | |
| B-3 | | 3,174 | | | | | | | |
| B-4 | | 3,277 | | | | | | | |
| B-5 | | | 3,484 | | | | | | |
| B-6 | | | 2,472 | | | | | | |
| B-7 | | | | | | | 2,543 | | |
| B-8 | | | | | | | 2,076 | | |
| B-9 | | | | | | | | 5,000 | |
| B-10 | | | | | | | | 5,402 | |
| B-11 | | | | | | | | | 5,060 |
| B-12 | | | | | | | | | 5,269 |

Average strength measured on the days
of start of dynamic tests = 3,747 psi

Note: The cap of cylinder was not used for tests done until cylinders B-6 and B-7

The modulus of elasticity of the concrete was obtained from the stress-strain relationship according to the procedure indicated by the ASTM (C-469).

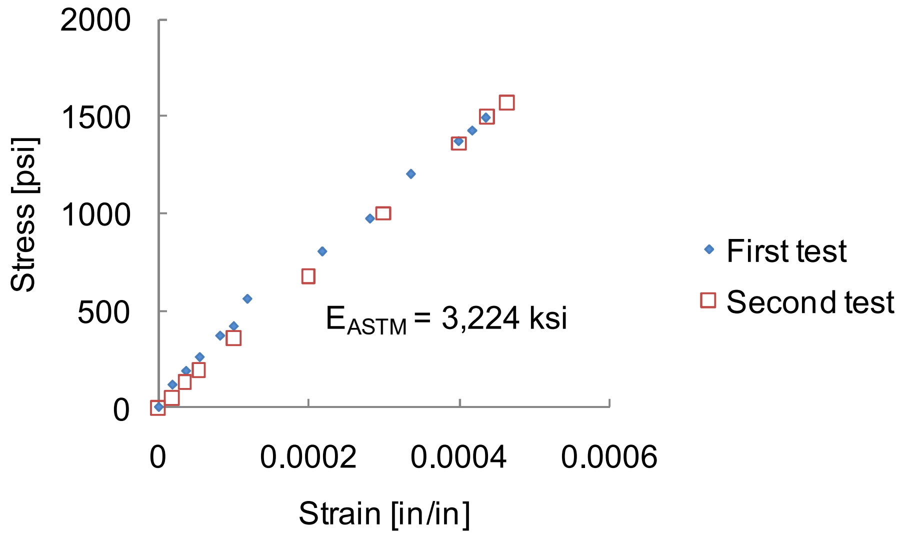


Figure E-1 Stress-strain relationship measured on cylinder A-9.

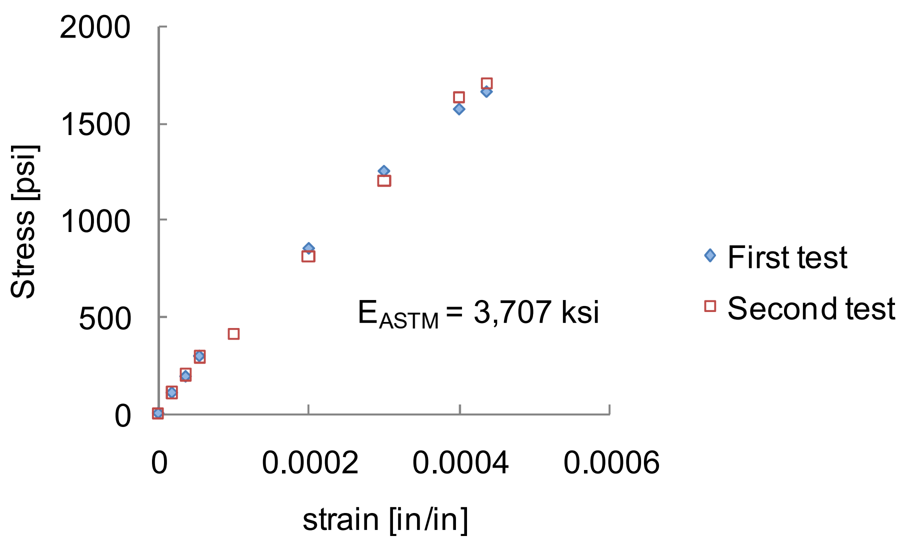


Figure E-2 Stress-strain relationship measured on cylinder A-10.

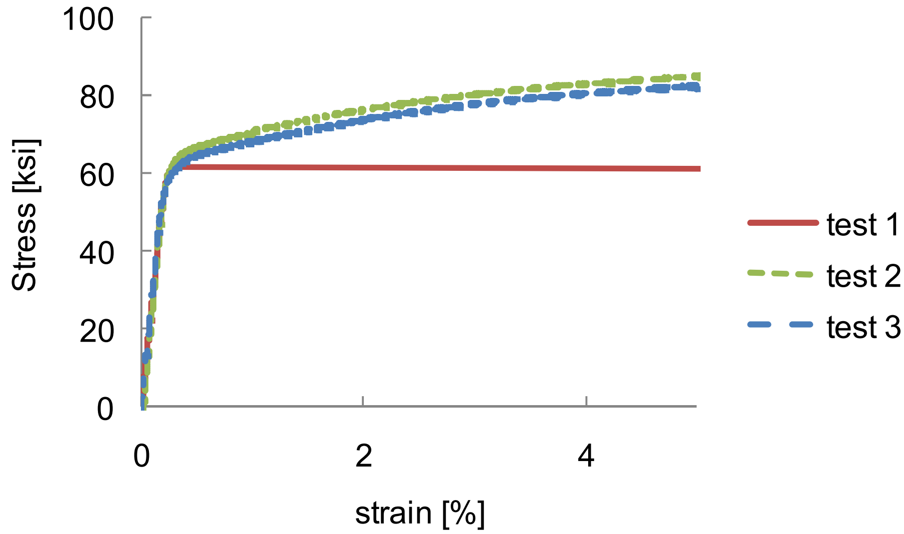


Figure E-3 Stress-strain relationship of longitudinal reinforcing bars.

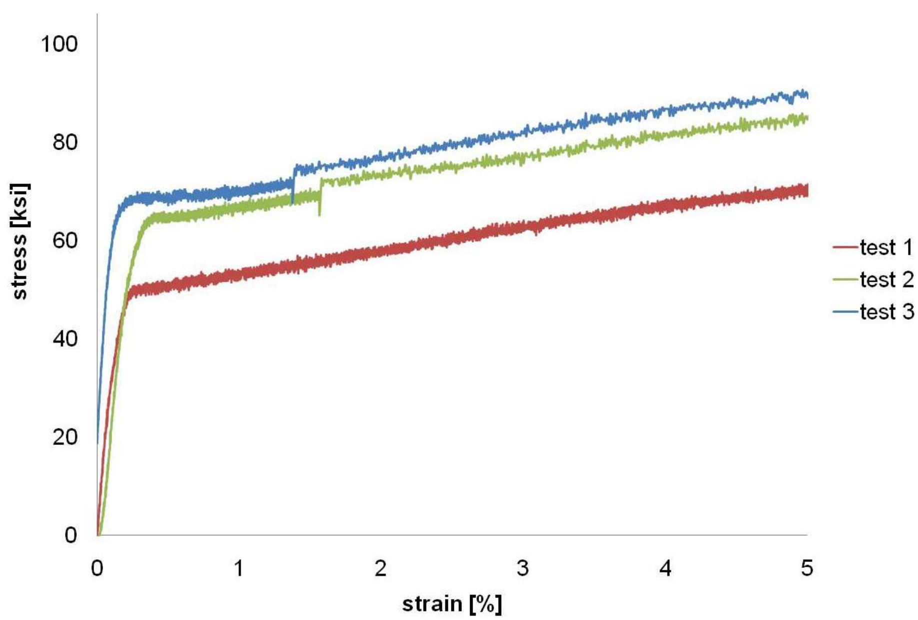


Figure E-4 Stress-strain relationship of transverse reinforcing bars.

Lateral load was applied at the beam tip in the pseudo-static tests by either spinning the nut (N) toward south direction (tension in the threaded rod), or by spinning the nut (S) toward north direction (compression in the threaded rod), depending on the direction of the cycle.

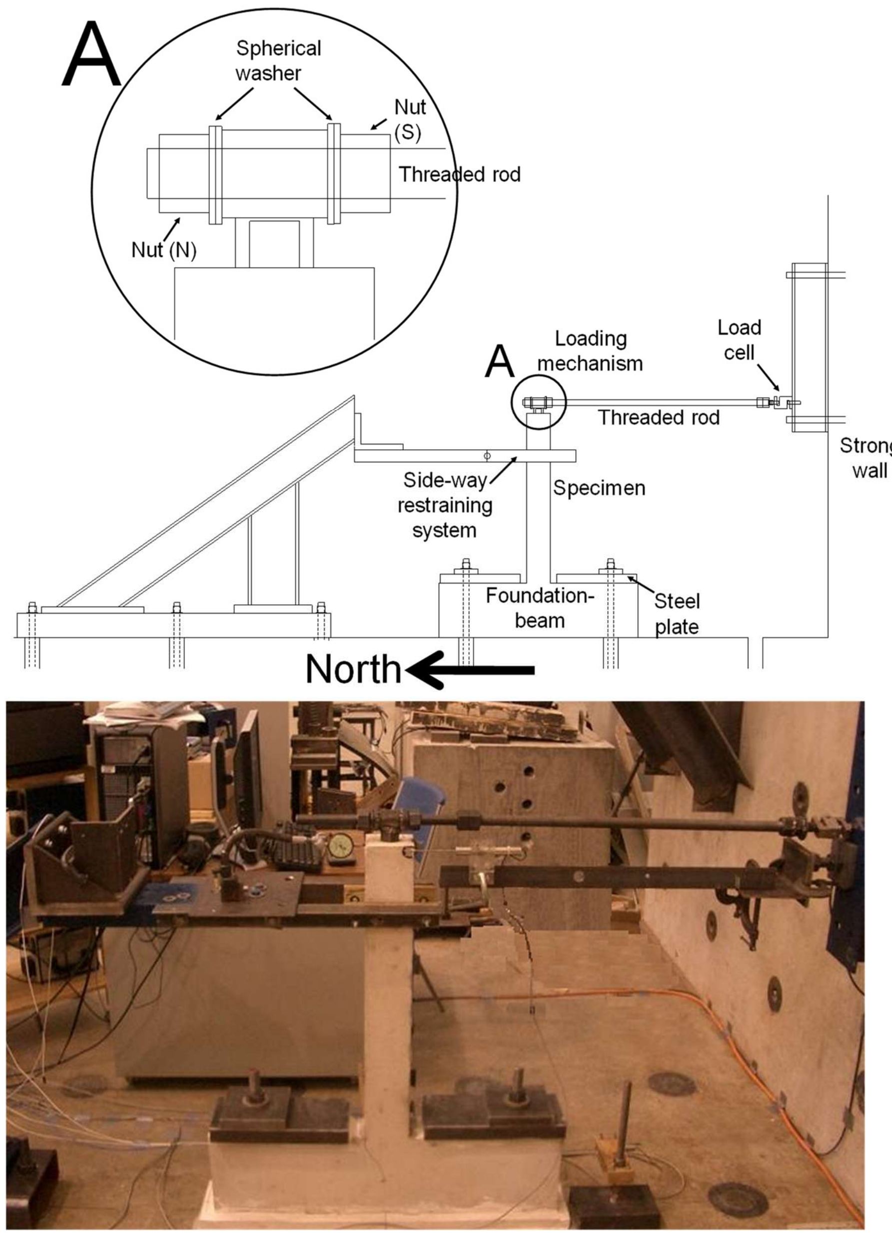


Figure E-5 Set-up of pseudo-static tests of small-scale specimens.

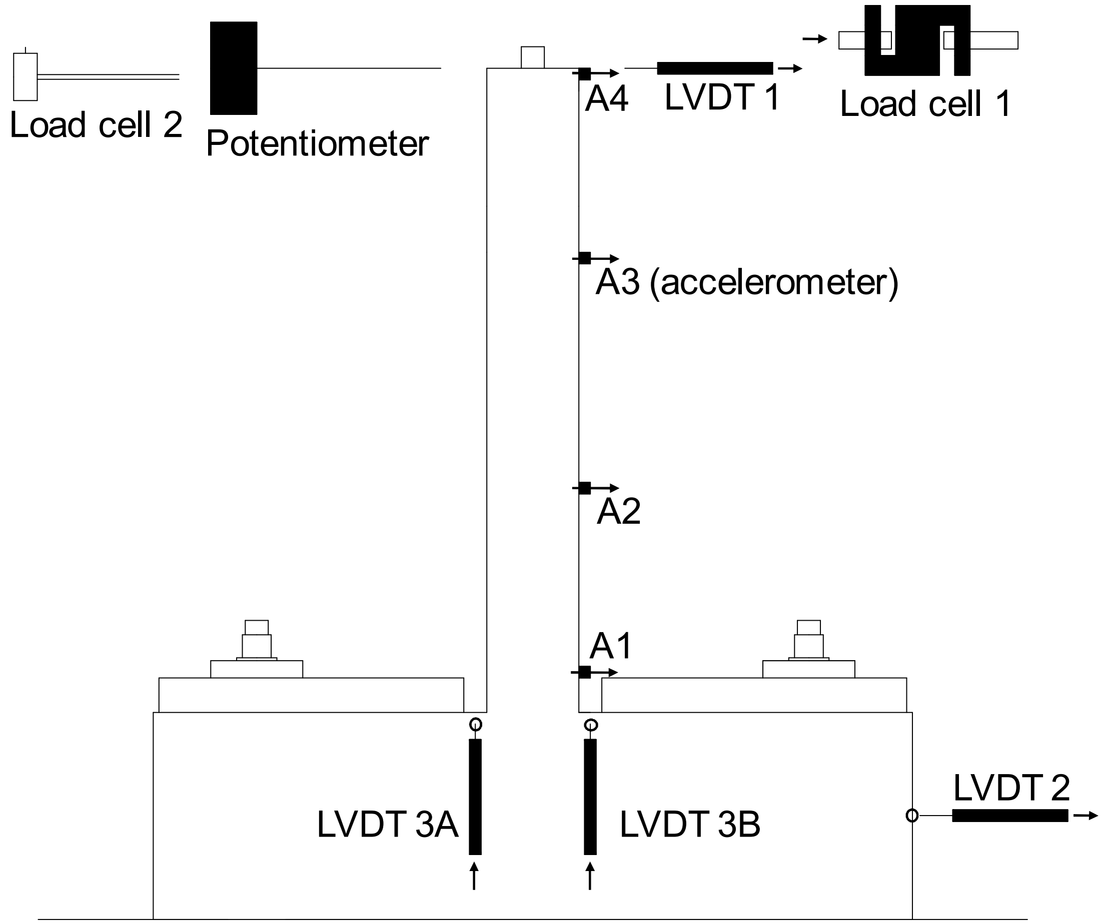


| Sensor | Sensitivity constant | units | Accuracy | Noise level |
|---|---|---|---|---|
| LVDT 1 | 20.258 | V/in | 0.001in | 3E-5in |
| LVDT 2 | 38.871 | V/in | 0.0005in | 3E-5in |
| LVDT 3A | 187.48 | V/in | 0.001in | 3E-5in |
| LVDT 3B | 96.958 | V/in | 0.001in | 3E-5in |
| A1 | 1,040 | mV/g | 0.08mg | 5.0mg |
| A2 | 1,060 | mV/g | 0.08mg | 5.0mg |
| A3 | 1,077 | mV/g | 0.08mg | 5.0mg |
| A4 | 1,000 | mV/g | 0.05mg | 1.0mg |
| Potentiometer | 0.4859 | V/in | 0.010in | 0.010in |
| Load cell 1 (static) | 0.01499 | V/kip | 0.75lbf | 0.5lbf |
| Load cell 2 (dyn.) | 0.4834 | V/lbf | 0.04lbf | 0.01lbf |

Figure E-6 Description and layout of sensors on the small-scale beams.

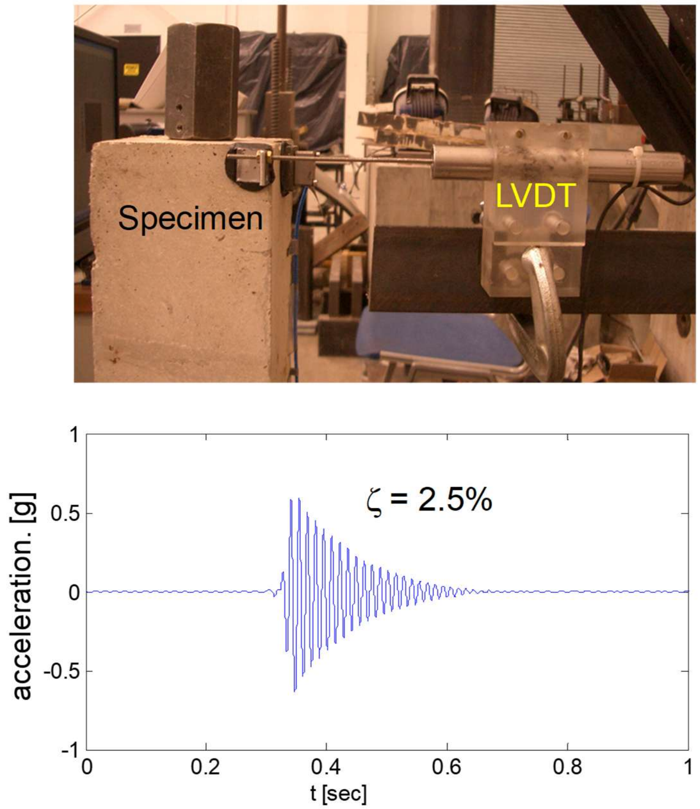


LVDT attached to the specimen

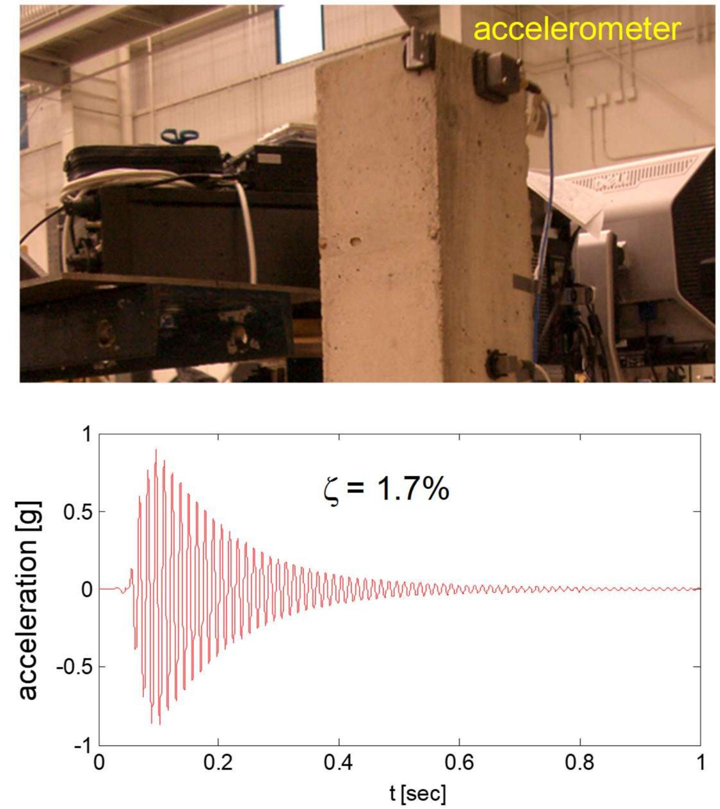


No LVDT attached to the specimen

Figure E-7 Comparison of free vibration with and without an LVDT attached to the specimen.

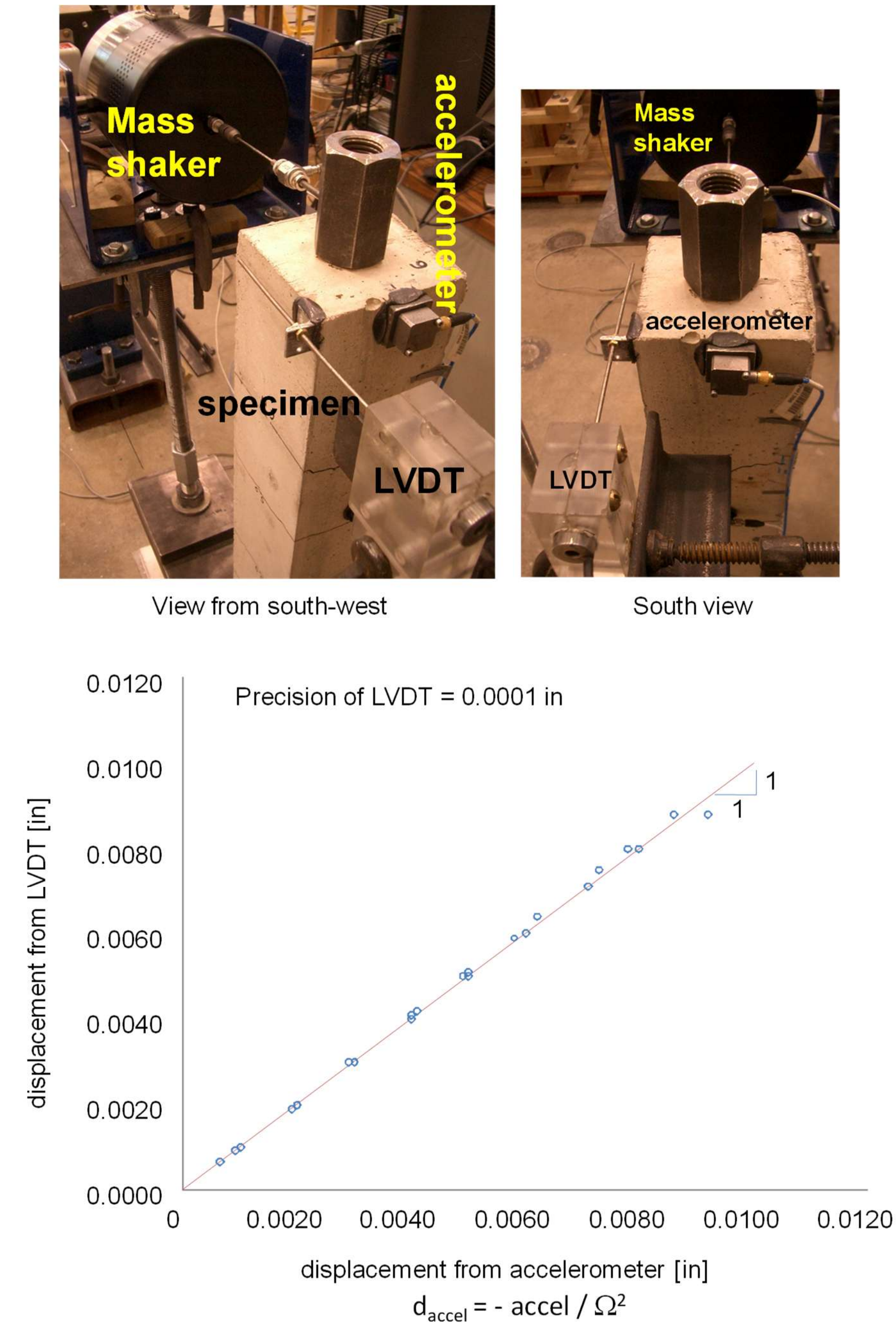


Figure E-8 Verification of displacement inferred from accelerations in the small-scale cantilever beams.

Crack surveying in the small-scale beams

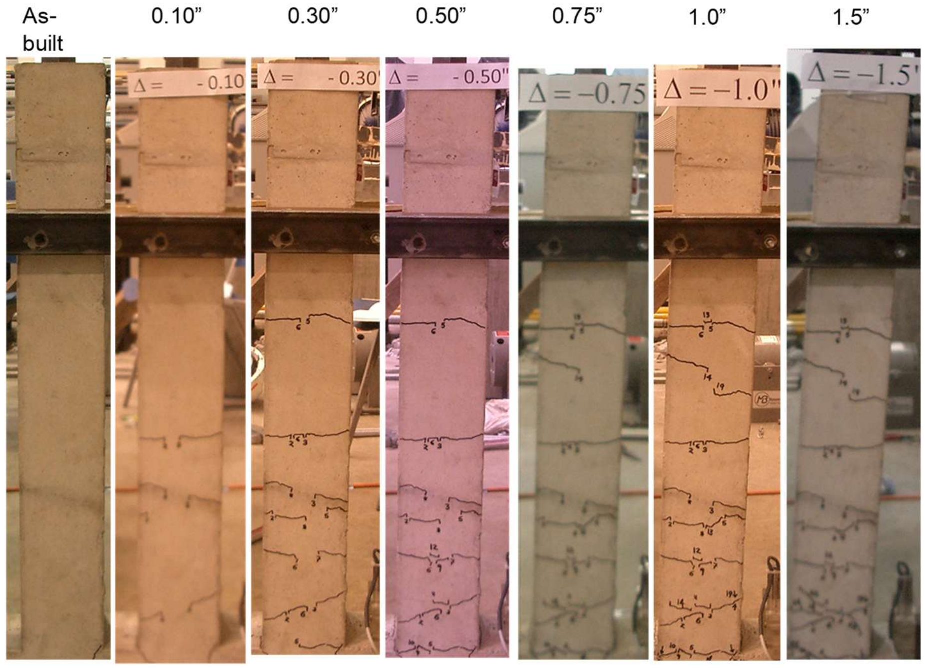


Figure E-9 Crack observation in Specimen 1

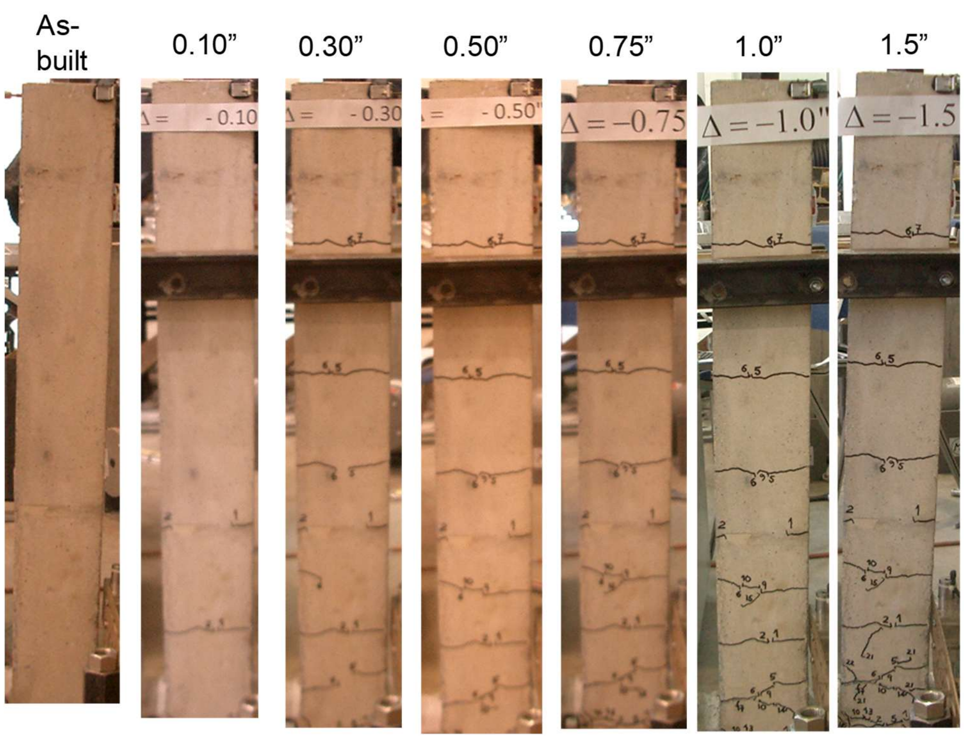


Figure E-10 Crack observation in Specimen 2

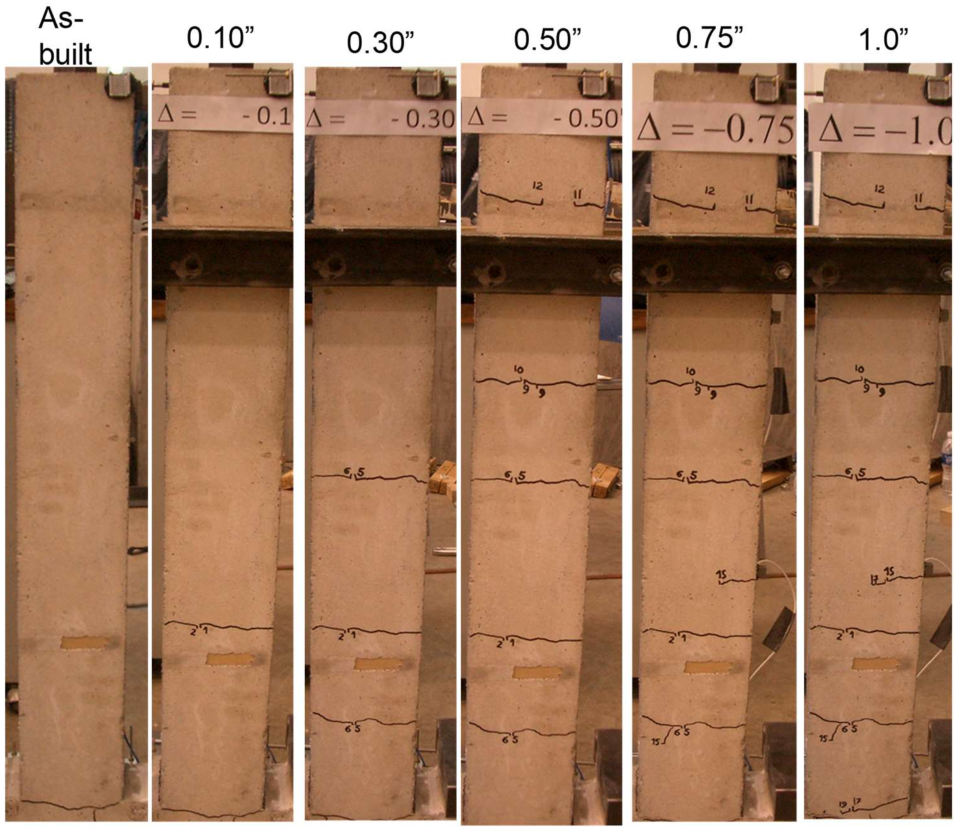


Figure E-11 Crack observation in Specimen 3

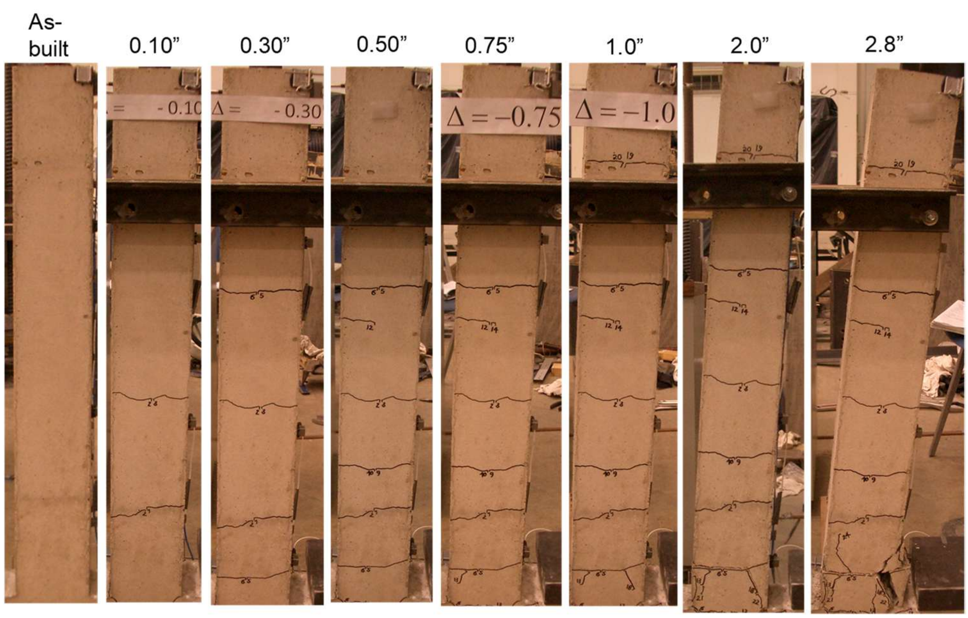


Figure E-12 Crack observation in Specimen 4

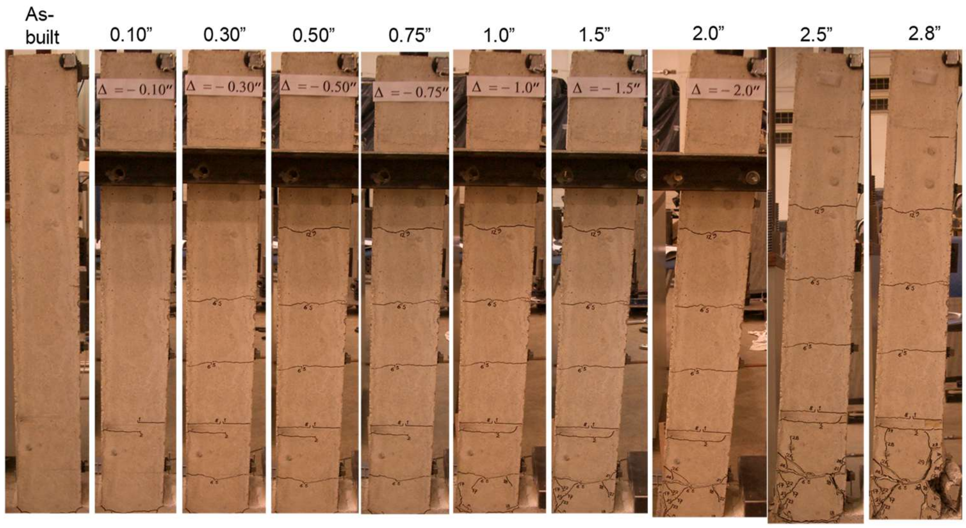


Figure E-13 Crack observation in Specimen 5

Maximum difference between damping estimates through forced and free vibration tests in small-scale beams was obtained for specimen 4. Such difference was obtained after 0.50 in displacement and initial displacement of 0.009 in ($\zeta$ = 22.7% from forced vibrations and $\zeta$ = 2% from free vibration). Figure E-14 (a) shows the acceleration response and the corresponding Fourier spectrum of the free vibration test. Damping estimated using peak 1 and peak 4 is more than 3 times the value in Table 4-13 ($\zeta_{1 \text{ to } 4}$ = 7%). The two frequency components (f = 30 Hz and f = 33 Hz) shown in Figure E-14 (b), make the signal to grow and decay with time producing inconsistent estimates of damping using logarithmic decrement.

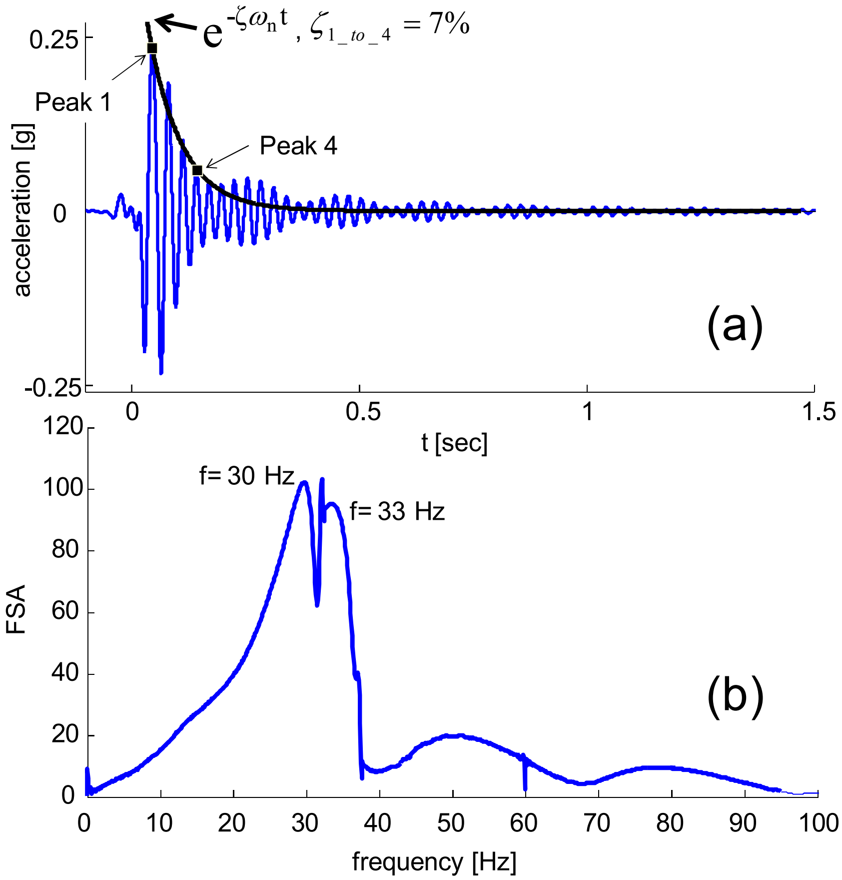


Figure E-14 Free vibration response for the case of maximum difference between damping estimates from free and forced vibration tests. (a) Acceleration response. (b) Fourier Spectrum.

Verification of sinusoidal input excitation during forced vibration tests on the small-scale beams was done by analyzing the frequency content of the acceleration response of the beam ($a_{top}$). Figure E-15 (c) and (d) illustrate the acceleration response ($a_{top}$), harmonic excitation load (P) and Fourier spectrum of the acceleration response (FSA of $a_{top}$) of tests labeled as 'a' and 'b' in the TF of Figure E-15 (a), respectively. Harmonic excitation is evidenced by the dominant peak in the FSA of $a_{top}$ corresponding to the excitation frequency ($f_a$ in Figure E-15 (c) and $f_b$ in Figure E-15 (d)).

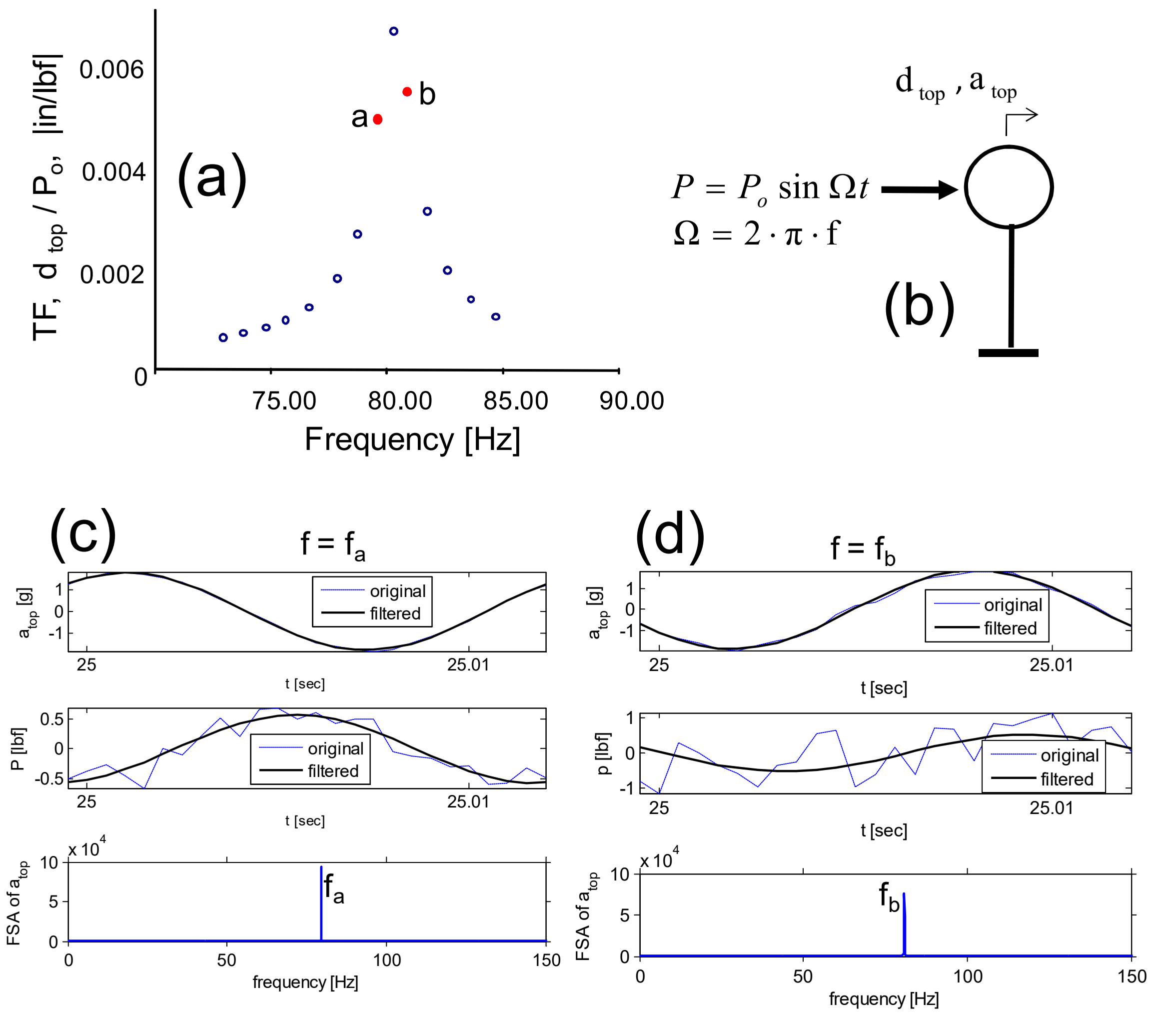


Figure E-15 Verification of harmonic excitation during forced vibrations on the small-scale beams.

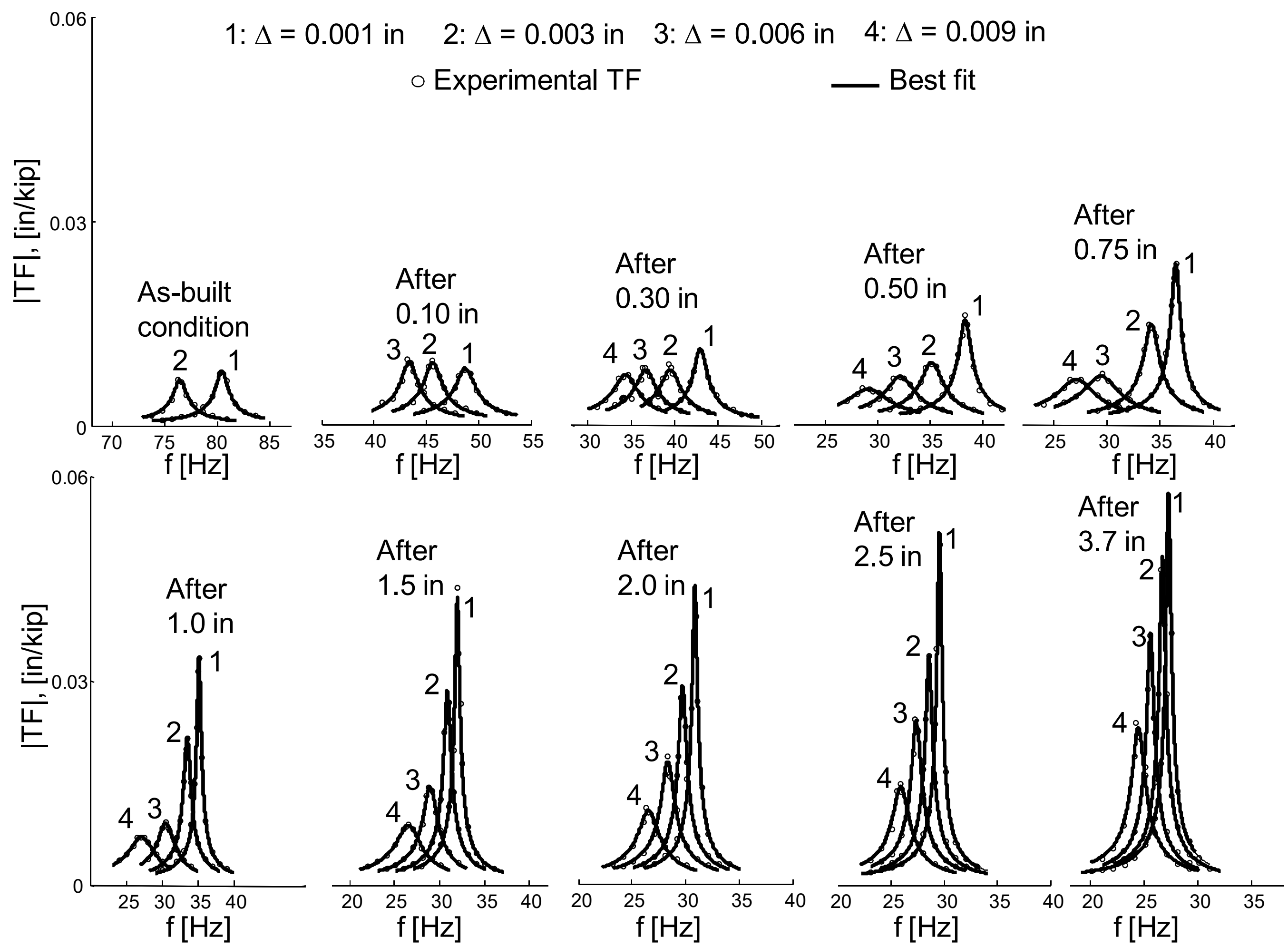


Figure E-16 Constant-displacement response transfer functions (TFs) for specimen 6.

Estimates of equivalent viscous damping ratio $\zeta$ under ambient vibrations reported in Table 4-21 and Table 4-22 were obtained by using "free vibration" portions of the ambient vibration records. Figure E-17 (a) and (b) show the acceleration ambient vibration record and the corresponding Fourier spectrum. Figure E-17 (c) shows the acceleration record for the time window marked by two dashed lines in Figure E-17 (a).

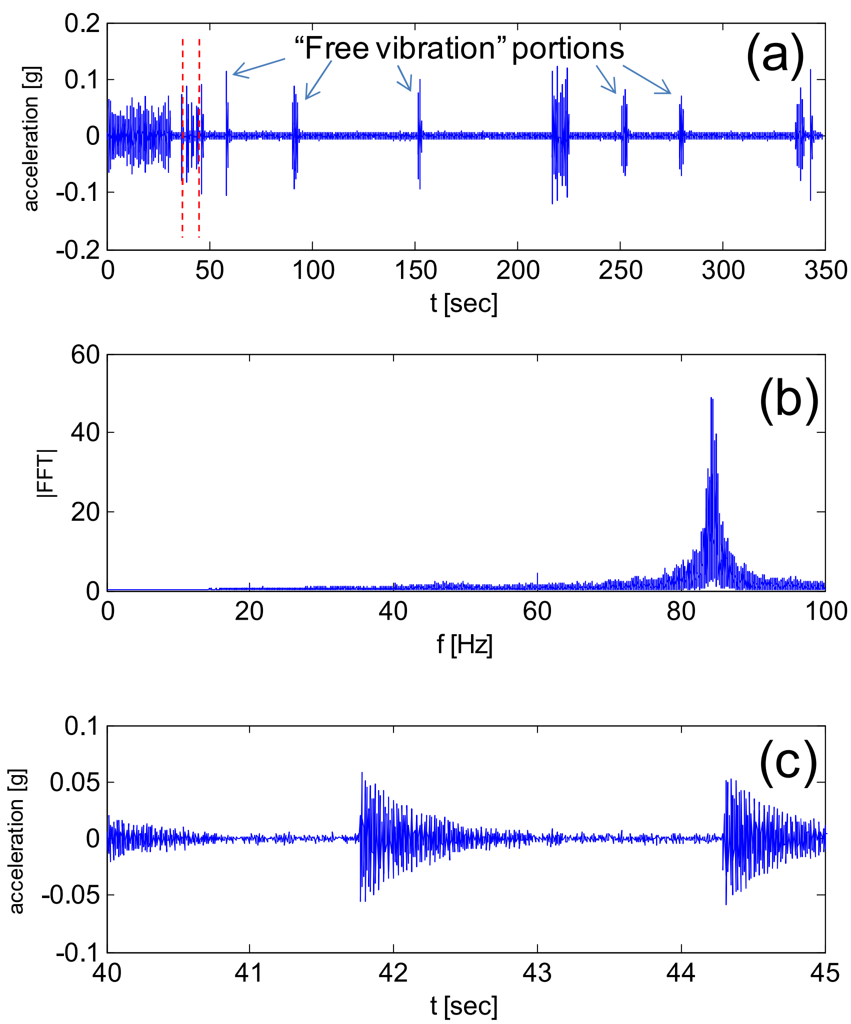


Figure E-17 "Free vibration" portions of ambient vibration records in the as-built condition of specimen 6. (a) Full record of ambient vibrations. (b) Fourier Spectrum. (c) Zoom-in to illustrate "free vibration" portions.

A constant-displacement response type of TF performed in the small-scale beams is equivalent to a "linearization" of the nonlinear elastic system. Figure E-18 (a) shows the FRF obtained by sweeping different frequencies and the corresponding estimates of frequency, damping and stiffness. Figure E-18 (b) shows the input force P(t), the output displacement x(t) and the resisting force for the case when the excitation frequency equals the natural frequency ($\Omega \sim \omega$). The damping estimate through the enclosed area by the resisting force versus displacement curve of Figure E-18 (c) is in good agreement with that of the FRF. The load versus displacement curve ($f_{spring}$-vs.-displ.) of Figure E-18 (c) computed according to the equations shown in the figure, is a straight line as a consequence of the "linearization" of the system by performing forced vibration tests with a constant displacement response.

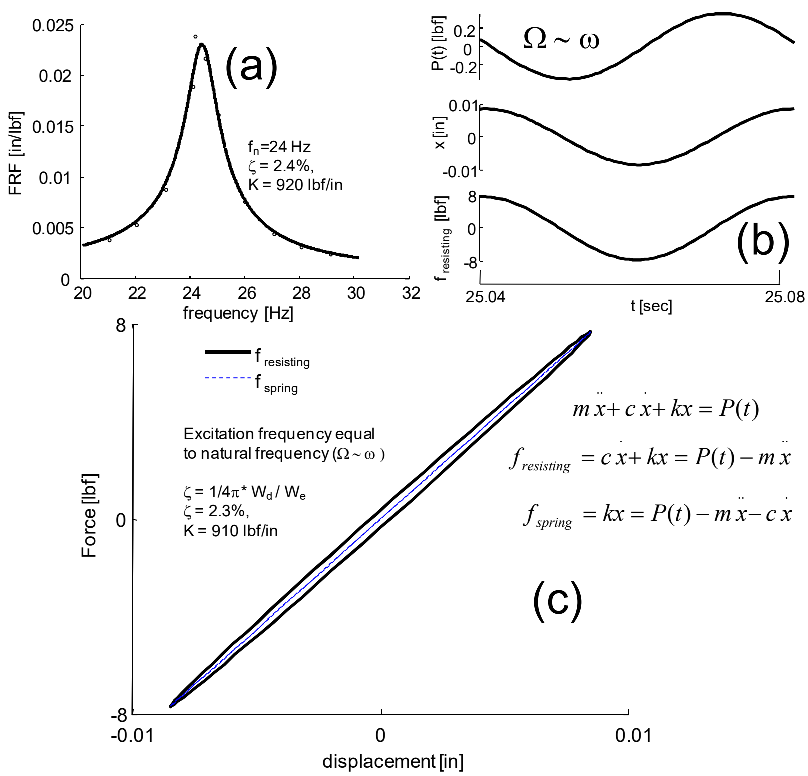


Figure E-18 "Linearization" effect of the forced vibration tests performed with constant displacement response. (a) FRF. (b) Input and output measurements when excitation frequency equals the natural frequency. (c) Force-displacement curve.

# Appendix F.
## Difference in damping estimates from free and forced vibration tests in the small-scale cantilever beams

In order to reconcile the difference in damping estimates from free and forced vibration tests performed at identical displacement levels (initial displacement of free vibration test equal to the displacement-amplitude response during steady-state of forced vibration tests), effect of variable stiffness and variable damping in the free vibration response was investigated. A SDOF system was defined with variable stiffness (from pseudo-static part of free vibration tests) and variable damping (from forced vibration tests) measured in experiments. The equivalent viscous damping was estimated using logarithmic decrement in the simulated response of the defined SDOF system. This estimate of equivalent viscous damping was compared to that observed in the actual free-vibration experiments.

The largest difference between damping estimates from free ($\zeta$ = 2.0%) and forced vibration ($\zeta$ = 22.7%) in the small-scale beams of chapter 4, was observed in specimen 4 in the condition after 0.50 in and measured at a displacement of 0.009 in (Table 4-13 and Table 4-20). An elastic SDOF system was defined with the variable stiffness and variable damping illustrated by the load-displacement curve and the damping-displacement relationship of Figure F-1 (a) and (b), respectively.

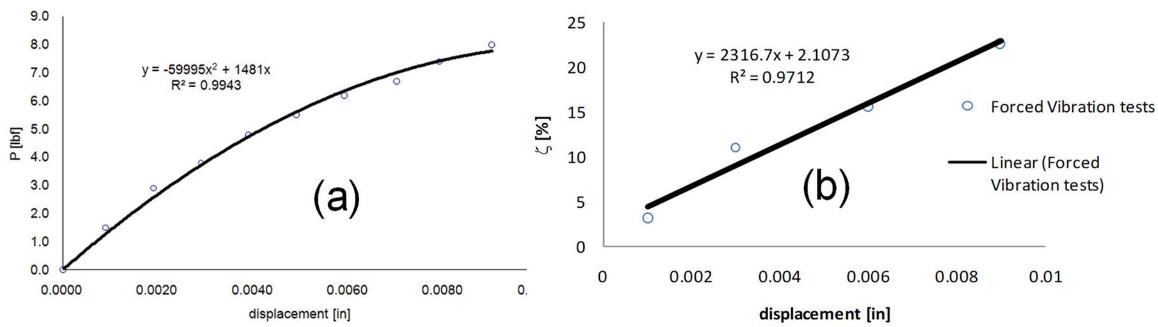


Figure F-1 Variable stiffness and variable damping of specimen 4 in the condition after 0.50 in. (a) Load versus displacement curve. (b) Equivalent viscous damping versus displacement.

The free vibration response of the defined SDOF simulated using an initial displacement equal to the displacement used in the experiments (0.009 in), is shown in Figure F-2. The system responds with an equivalent viscous damping ratio of about $\zeta$ = 23% at the beginning of the free vibration response (as defined for a displacement of 0.009 in). However, a totally different estimate of damping is obtained using logarithmic decrement after 40 cycles ($\zeta_{1 \text{ to } 40}$ = 2.6%). Actual estimate of equivalent viscous damping ratio using logarithmic decrement from free vibration experiments after 40 cycles is $\zeta_{1 \text{ to } 40}$ = 2.0% (Table 4-13).

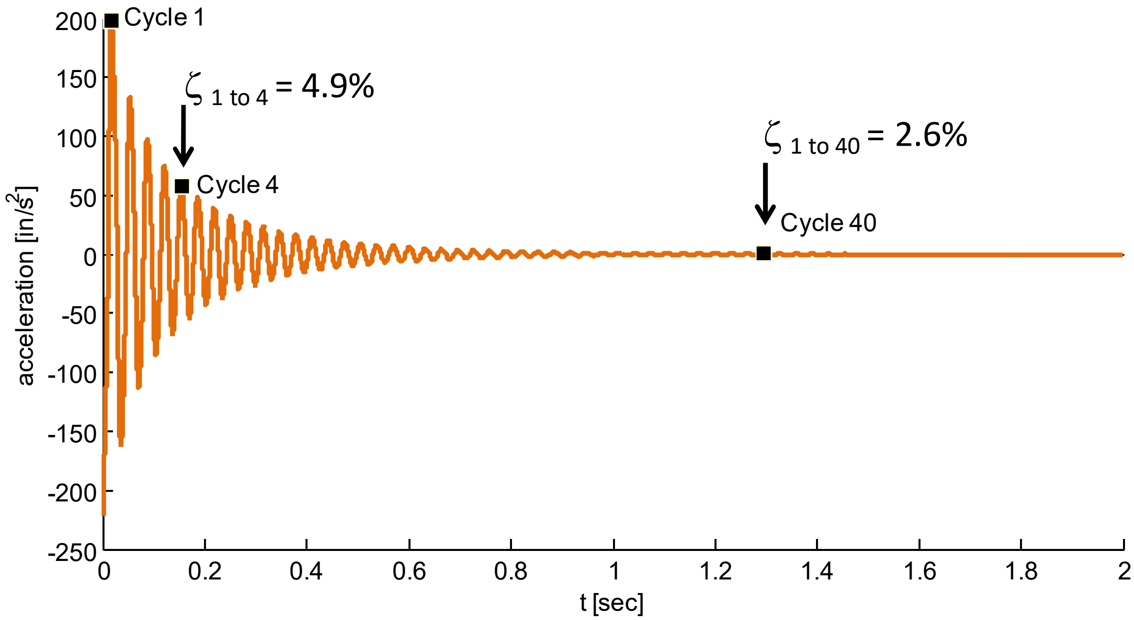


Figure F-2 Free vibration response of an elastic SDOF defined with variable stiffness and variable damping observed in specimen 4.

Similar investigation of discrepancy between damping estimates from free and forced vibration tests was done for specimen 5. The largest difference between damping estimates from free ($\zeta$ = 1.4%) and forced vibration ($\zeta$ = 10.9%) in specimen 5, was observed in the condition after 0.75 in measured at a displacement of 0.009 in (Table 4-14 and Table 4-21). An elastic SDOF system was defined with the variable stiffness and variable damping illustrated by the load-displacement curve and the damping-displacement relationship of Figure F-3 (a) and (b), respectively.

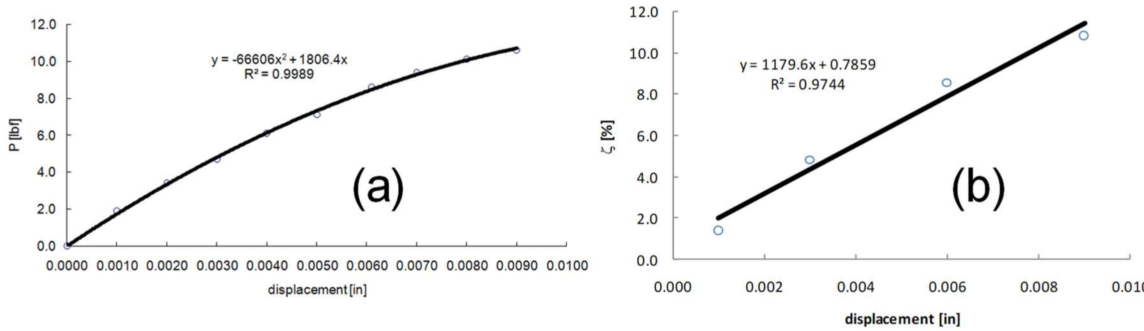


Figure F-3 Variable stiffness and variable damping of specimen 5 in the condition after 0.75 in. (a) Load versus displacement curve. (b) Equivalent viscous damping versus displacement.

The free vibration response of the defined SDOF simulated using an initial displacement equal to the displacement used in the experiments (0.009 in), is shown in Figure F-4. The system responds with an equivalent viscous damping ratio of about $\zeta$ = 11% at the beginning of the free vibration response (as defined for a displacement of 0.009 in). However, a totally different estimate of damping is obtained using logarithmic decrement after 40 cycles ($\zeta_{1\text{ to }40}$ = 1.3%). Actual estimate of equivalent viscous damping ratio using logarithmic decrement from free vibration experiments after 40 cycles is $\zeta_{1\text{ to }40}$ = 1.4% (Table 4-14)

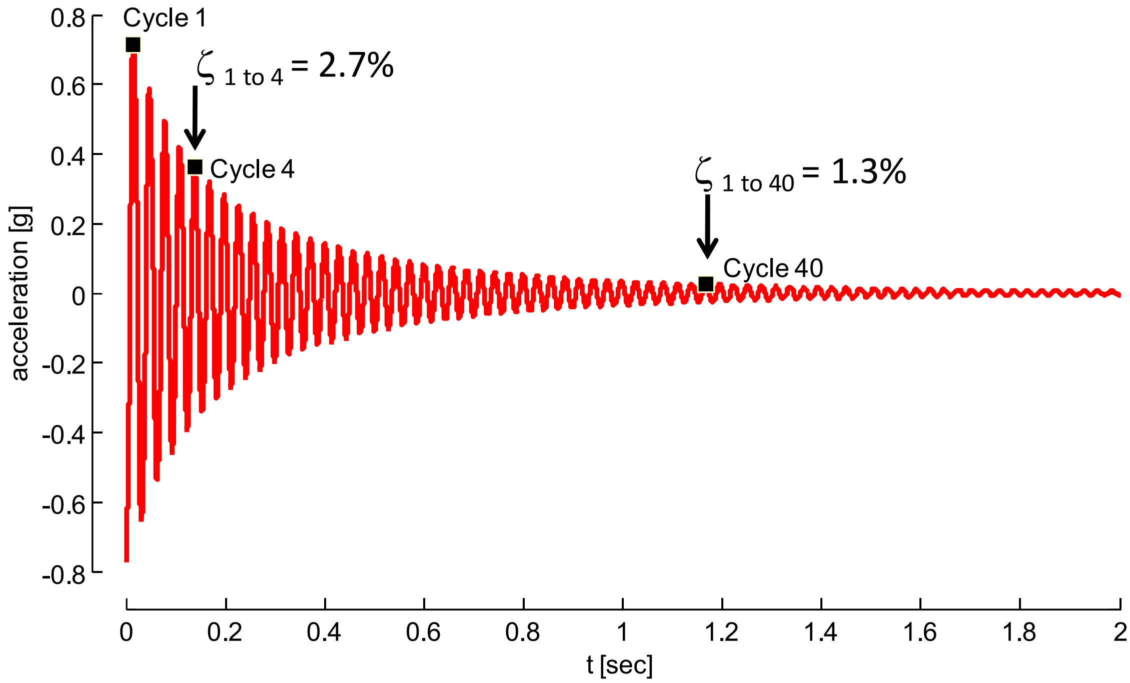


Figure F-4 Free vibration response of an elastic SDOF defined with variable stiffness and variable damping observed in specimen 5

# Appendix G.

## Lateral displacement of full-scale 3-story flat-plate building to cause crack of the column

$fc := 4000psi$

$E := 57000 \cdot \sqrt{\frac{fc}{psi}} psi \qquad E = 3.605 \times 10^{3}\, ksi$

$b := 18in \qquad h := 10ft$

$Ig := \frac{1}{12} \cdot b^{4}$

$k := \frac{12 \cdot E \cdot Ig}{h^{3}}$

$\sigma axial := 0.05 \cdot fc$

$\sigma cr := 0.10 \cdot fc$

Consider the superposition of axial load and bending due to lateral displacement

$\Delta cr := \frac{4 \cdot Ig}{k \cdot h \cdot b} \cdot (\sigma cr + \sigma axial) \qquad \Delta cr = 0.044\, in$

$drift := \frac{\Delta cr}{h} \qquad drift = 0.04\,\%$

Assume linear variation of displacement with height

$\Delta roof := 3 \cdot \Delta cr \qquad \Delta roof = 0.13\, in$

# Appendix H.

## Comparison of actual and simulated responses of different amplitudes in the full-scale 3-story flat-plate building

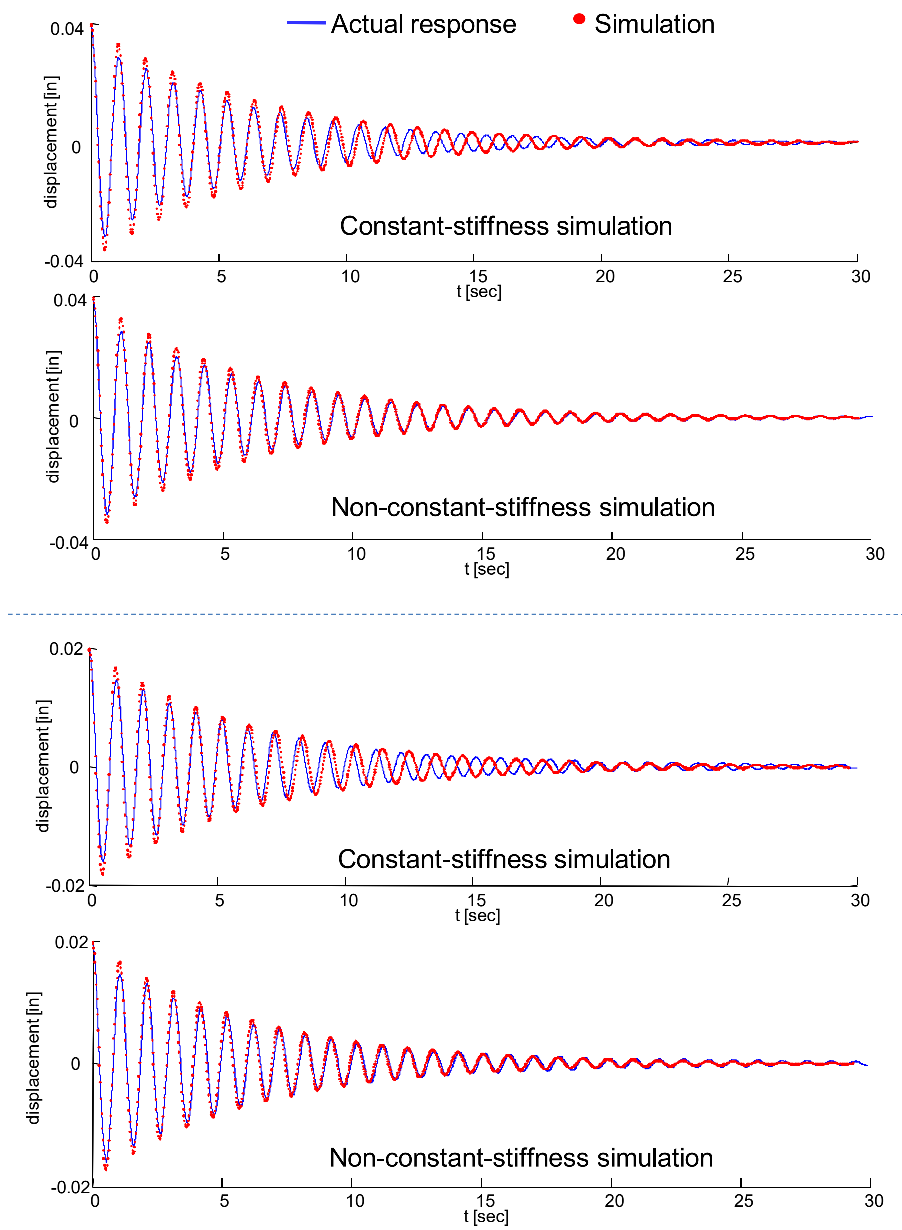


Figure H-1 Nonlinear-elastic behavior of the full-scale structure under free vibrations.

# Appendix I.

## Lateral displacement to cause crack in the small-scale cantilever beams

$h := 28in \quad b := 4in \quad t := 4in \quad fc := 3200psi \quad fy := 66ksi$

$Ec := 57000 \cdot \sqrt{\frac{fc}{psi}}\, psi \qquad Ec = 3224 \cdot ksi$

$Es := 29000ksi \qquad n := \frac{Es}{Ec}$

$I := \frac{1}{12} \cdot b \cdot t^3 \qquad I = 21.3 \cdot in^4$

$k := \frac{3Ec \cdot I}{h^3} \qquad k = 9.4 \cdot \frac{kip}{in}$

Cracking Point

$\sigma cr := 7.5 \cdot \sqrt{\frac{fc}{psi}}\, psi \qquad \sigma cr = 424 \cdot psi$

$Mcr := \frac{2\sigma cr \cdot I}{t} \qquad Mcr = 4.5 \cdot kip \cdot in$

$\phi cr := \frac{Mcr}{Ec \cdot I} \qquad \phi cr = 6.579 \times 10^{-5} \cdot \frac{rad}{in}$

Lateral Load and Displacement to crack specimen

$Pcr := \frac{Mcr}{h} \qquad Pcr = 162 \cdot lbf$

$\Delta cr := \frac{Pcr}{k} \qquad \Delta cr = 0.017 \cdot in \qquad \frac{\Delta cr}{h} = 0.06 \cdot \%$

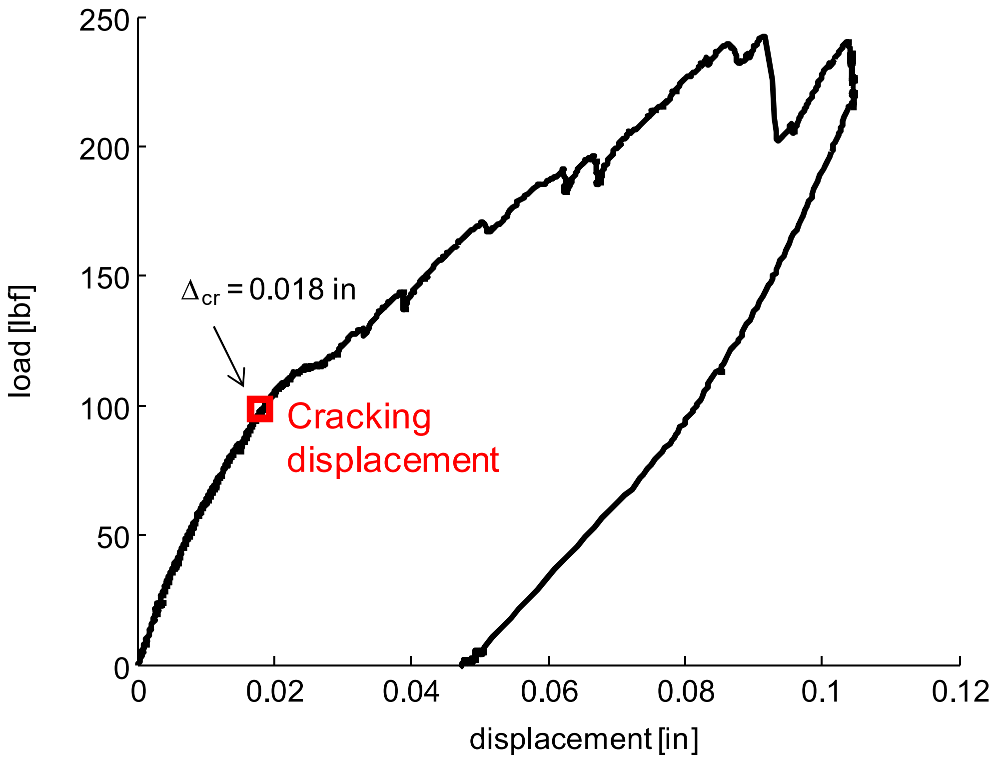


Figure I-1 Illustration of the cracking displacement of specimen 6 in the pseudo-static test.

# Appendix J.

## Axial stresses in the columns of the full-scale 3-story building under small-amplitude vibrations

$fc := 4500 \cdot psi$

$H := 30 \cdot ft \qquad b := 18 \cdot in$

$L := 20 \cdot ft$

$$M := \begin{pmatrix} 0.401 & 0 & 0 \\ 0 & 0.401 & 0 \\ 0 & 0 & .401 \end{pmatrix} kip \cdot \frac{s^2}{in}$$

$$\phi := \begin{pmatrix} 0.25 \\ 0.68 \\ 1.00 \end{pmatrix}$$

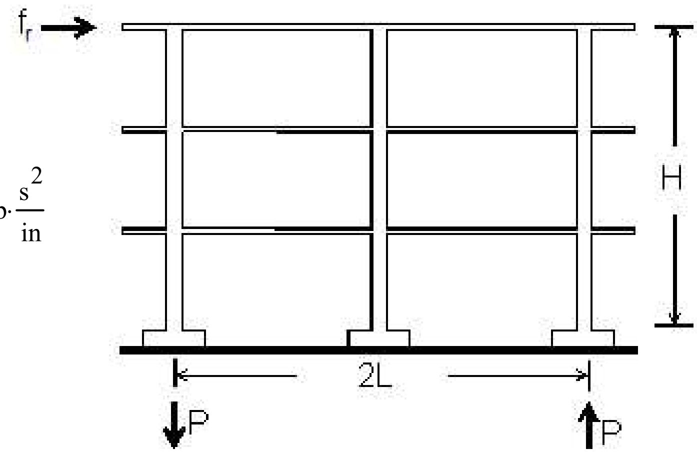


Equivalent mass at the top of the building

$Meq := \phi^T \cdot M \cdot \phi \qquad Meq = 2.361 \times 10^5 \cdot lb$

Original natural frequency

$f := 1.98 \cdot Hz \qquad \omega := 2 \cdot \pi \cdot f$

$d := 0.10 \cdot in$ (limit of small-amplitude vibrations)

$accel := (2 \cdot \pi \cdot f)^2 \cdot d \qquad \dfrac{accel}{g} = 0.04$

Resisted force by the system during small-amplitude vibrations

$fr := Meq \cdot accel \qquad fr = 9.5 \cdot kip$

Axial load and stress in the building column caused by small-amplitude vibrations

$P := \dfrac{fr \cdot H}{2 \cdot L} \qquad P = 7.1 \cdot kip$

$\sigma axial := \dfrac{P}{3 \cdot b^2} \qquad \sigma axial = 7 \cdot psi$

Axial stress due to gravity loads in the building

$\sigma axial\_2 := \dfrac{500 \cdot kip}{6 \cdot b^2} \qquad \sigma axial\_2 = 257 \cdot psi \qquad \boxed{\dfrac{\sigma axial\_2}{fc} = 0.06}$

# Appendix K.

## Small-scale structures of Table 6-1

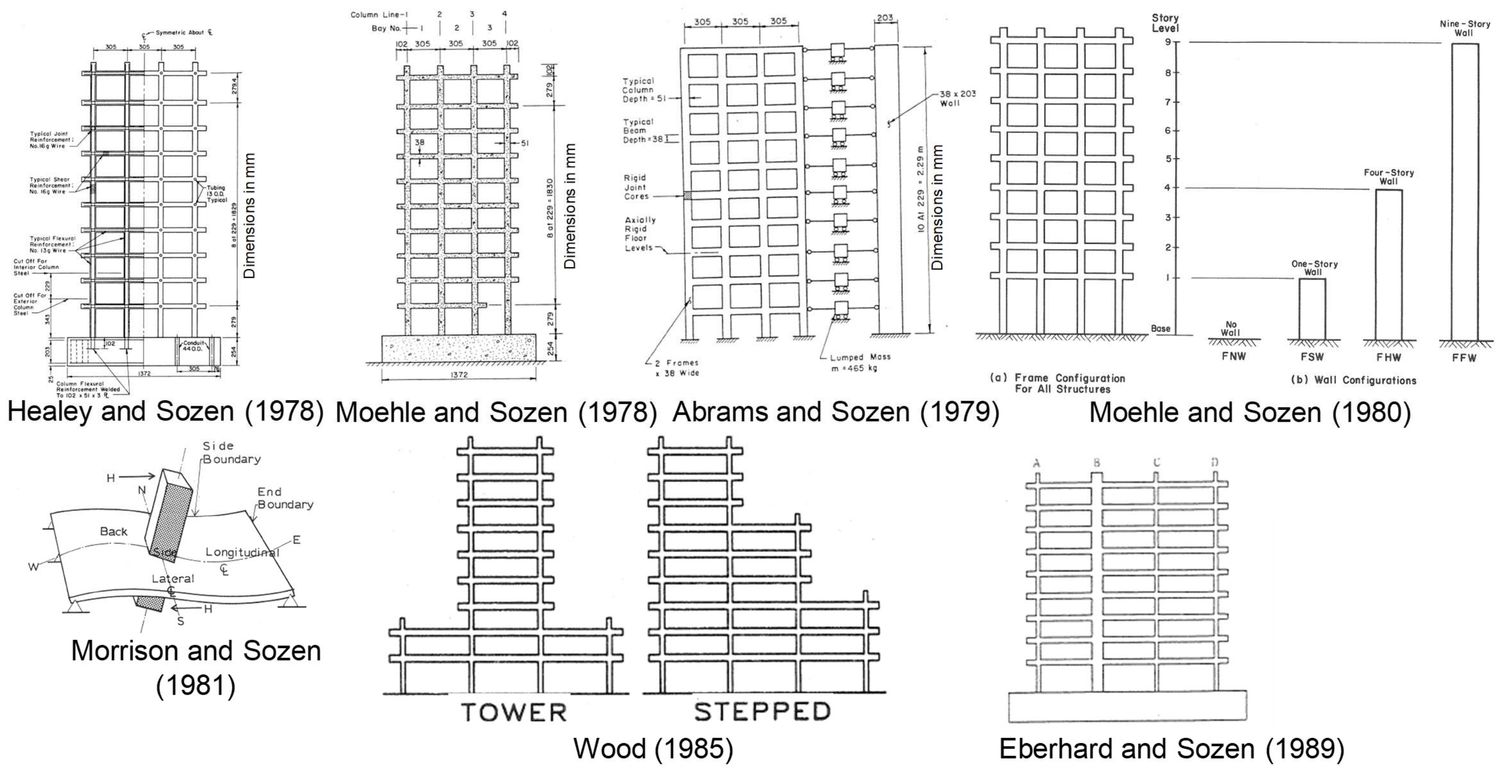


Figure K-1 Small-scale structures of Table 6-1

# Appendix L.

## Displacement amplitudes of free-vibration tests on specimens tested by Eberhard and Sozen (1989)

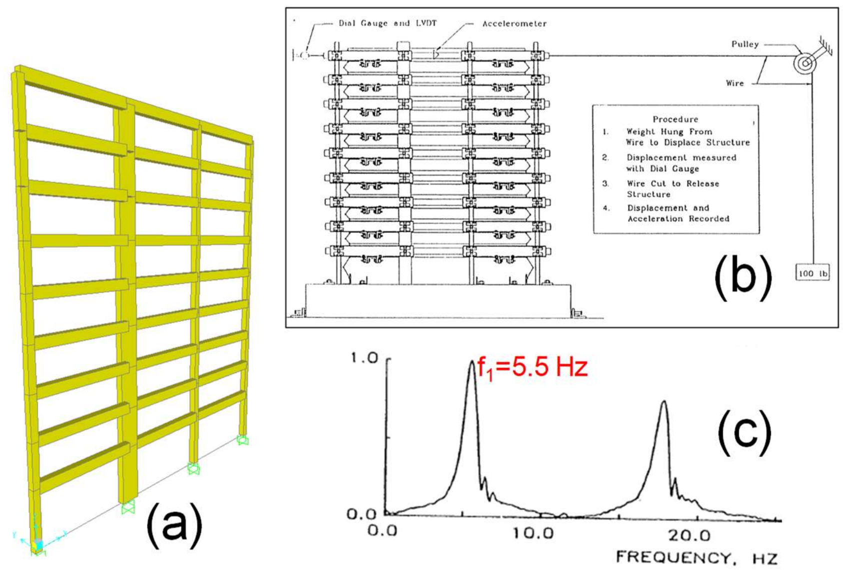


Estimation of displacement amplitudes during free vibration tests using finite element model:

The finite element model built using gross section properties was verified by comparing the estimated natural frequency versus the measured natural frequency in the as-built condition ($f_1$ = 5.5 Hz). The initial displacement of the free-vibration tests was estimated as the displacement caused by the force used in the tests (P = 100 lbf), applied to the "verified" finite element model.

Gross properties → $f_1$= 5.3 Hz , $K_{top}$ = 6.5 kip/in,
$\Delta_{top}$ = 0.015 in
(**0.02%** drift for P = 100 lbf)

Final condition → $f_{end}$ = 2.1Hz, $K_{top}$ = 0.9 kip/in,
$\Delta_{top}$ = 0.11 in
(0.12% drift for P = 100 lbf)

Figure L-1 Estimates of displacement amplitudes on the specimen tested by Eberhard and Sozen (1989) using a finite element model. (a) Finite element model. (b) Free-vibration test set-up. (c) Fourier Spectrum measured in the as-built condition.

VITA